

ADDIS ABABA UNIVERSITY
SCHOOL OF GRADUATE STUDIES

**GEOPHYSICAL INVESTIGATIONS FOR LAKE LEVEL
RISE STUDIES, NORTHERN PART OF LAKE BESEKA**

BY
BERIHUN ASFAW AREGGA

JUNE, 2001



**GEOPHYSICAL INVESTIGATIONS FOR LAKE LEVEL
RISE STUDIES, NORTHERN PART OF LAKE BESEKA**

**A Thesis submitted to the School of Graduate Studies
of Addis Ababa University in partial fulfillment
for the Degree Master of Science in Geophysics**

BY

BERIHUN ASFAW AREGGA

JUNE, 2001

ACKNOWLEDGMENT

My acknowledgment goes first and for most to my advisors, Dr. Tigistu Haile and Dr. Getinet Mewa, whose unreserved and proper advisees make me to finish the research on time.

I would like to express my deepest appreciation to the Geophysics Department staff members of the Ethiopian Geological Survey, Ato Shimelis Belayneh, Ato Getachew Burussa and W/o Anisha Mohammed for their enormous help to bring this work to an end.

I am also greatly indebted to my friends Ato Desalegn Mehiret who provides me computer facility at his home and Ato Berihanu Wudu for his generosity in typing the theisis taking his precious time.

I extend my gratitude to Water Works and Design Enterprise particularly to Ato Enigida Zemedikun for providing me all the necessary information regarding the study area

TABLE OF CONTENTS

	pages
ACKNOWLEDGMENTS	I
CONTENTS	II
LIST OF FIGUERS	V
ABSTRACT	VI
1 INTRODUCTION	1
1.1 The Study Area	1
1.1.1 Location and Accessibility	1
1.1.2 Climate	1
1.2 Previous Geophysical work	3
1.3 Objectives of the present study	5
1.4 Methodology	5
2 GEOLOGY, TECTONICS AND SEISMIC ACTIVITY	7
2.1 GEOLOGY	7
2.1.1 Regional Geology of the Study Area	7
2.1.2 Local Geology of Lake Beseka and its surrounding	8
2.2 Tectonic Features Underlying Lake Beseka and its surrounding	10
2.3 Effects of Seismic Activity on Beseka Lake Level Rise	12
3 THE ELECTRICAL RESISTIVITY METHOD: BASIC THEORY AND MATHEMATICAL FOUNDATIONS	14
3.1 Introduction	14
3.2 Earth Resistivity	15
3.2.1 Basic Idea and Scope	15

3.2.2	Current Flow and Potential Distribution over a Homogenous Earth	15
3.2.3	A Point Source of Current over a Semi-Infinite Homogenous	17
3.2.4	Two Sources of Current over a Semi-Infinite Medium	19
3.3	Apparent Resistivity	21
4	INSTRUMENTATION ELECTROD LAYOUTS AND FIELD PROCEDURES INTERPRETAION, DATA PROCESSING AND PRESENTATION	22
4.1	Instruments Used for Vertical Electrical Sounding (VES) Survey	22
4.2	Electrodes Layouts and Field Procedures	23
4.3	Instrumentation of Vertical Electrical Sounding Data	25
4.3.1	Curve Matching by Master Curves	25
4.3.2	Partial Curve Matching	26
4.4	Data Processing and Presentation	27
5	BASIC THEORY AND FIELD SURVEY OF THE MAGNETIC SURVEY	29
5.1	Introduction	29
5.2	Fundamental Principles of the Magnetic Method	30
5.3	Earth's Magnetic Field	32
5.3.1	Elements of the Earth's Magnetic Field	32
5.3.2	Origin of the Geo-Magnetic (or Total) Field	33
5.3.2.1	The Main Field	34
5.3.2.2	The External Magnetic Field	34
5.3.2.3	Local Magnetic Anomalies	35

5.4	Instrumentation and Field Procedure	36
5.5	Instrumentation of Magnetic Data	36
6	GEOPHYSICAL RESULTS	38
6.1	Vertical Electrical Sounding (VES) Results	38
	6.1.1 Profile One	38
	6.1.2 Profile Two	40
	6.1.3 Profile Three	42
	6.1.4 Profile Four	46
	6.1.5 Profile Five	49
6.2	Magnetic Results	54
7	CONCLUSIONS AND RECOMMENDATIONS	60
7.1	Conclusions	60
7.2	Recommendation	61
	REFERENCES	63

LIST OF FIGURES		Page
Fig.1	Location Map of the lake Beseka	2
Fig.2	Geological Map of Lake Beseka	90
Fig.3	Distribution of Current in a Semi-Infinite Medium due to a point Source of Current	17
Fig.4	The Current and Two Potential Electrodes On the Surface A Homogeneous Isotropic Ground	19
Fig.5	The Schlumberger Electrode Configuration	24
Fig.6	Elements of the Earth's Magnetic Field	35
Fig.7	Geoelectric section Along Line LV ₁	39
Fig.8	Geoelectricsection Along Line LV ₃	41
Fig.9	Apparent Resistivity Pseudosection Along Line Lv ₂	43
Fig.10	Geoelectric Section Along Line Lv ₃	44
Fig.11	Apparent Resistivity Pseudosection Alongline Along Line LMV ₃	47
Fig.12	Geoelectricsection Along LineLMV ₄	48
Fig.13	Apparent Resistivity Pseudosection Alongline LMV ₄	50
Fig.14	Geoelectricsection Along LineLMV ₅	51
Fig.15	Apparent Resistivity Pseudosection Alongline LMV ₅	53
Fig.16	Total Field Magnetic Anomally Profile Along Line LMV ₁	55
Fig.17	Total Field Magnetic Anomally Profile Along Line LMV ₂	56
Fig.18	Total Field Magnetic Anomally Profile Along Line LMV ₂ LMV ₄ (a), LMV ₄ (b), LMV ₅ (c)	57
Fig.19	Total Field Magnetic Map of Methehara Area	59

ABSTRACT

Geophysical methods provide the tools for solving various geological problems. In the case of this work, vertical electrical sounding (VES) and magnetic methods are carried out in the vicinity of Lake Beseke. The site is situated at about 200 km east of Addis Ababa near the town of Methahara. The study is performed in connection with M.SC research training to appreciate the effectiveness of the methods used and on the one hand it contributes additional data to obtain the subsurface information that has been contributing to the lake level rise.

The variation of resistivity with depth is studied by a progressive increase of the Schlumberger current electrode configuration using PASI-16GL earth resistivity meter and PASI-P300 energizer. In order to get a reasonable subsurface information, the apparent resistivity curve plotted in the field had been compared with a set of theoretically calculated master curves. The layer parameters, resistivity and thickness, obtained by iteration processes were used to construct geoelectric sections for each profile to show different lithological units in the vertical direction.

In addition to VES, the magnetic survey was carried out using scintrex made proton precession magnetometer (IGS-MP-3/4) and monitored with a selected base station for diurnal correction. The magnetic survey is applied to delineate subsurface structures (faults/shear zones), which have been created due to the tectonic activities taking place in the area. As shown from the total field magnetic map (fig.19), the northwestern part of the lake is characterized by exposed or shallow depth volcanic rocks. But the northeastern part of the lake is generally seems to be magnetically quite. The NNW and SSE inferred

fault may intersect the NNE-SSW trending fault through which the thermal springs apparent in the area may come to the surface.

The results of the Vertical electrical sounding surveys show that the resistivity of the different aquifer systems is low in the vicinity of the lake and increases away because of the intrusion of the saline lake water. It has been found that no input of water to the lake is possible from the adjacent farmlands, as the water table gets deeper as one goes away from the lake.

1. INTRODUCTION

1.1 THE STUDY AREA

1.1.1 Location and Accessibility

The study area is located in the Oromiya region, 200km east of Addis Ababa, near Metahara town, on the Addis Ababa–Asseb highway (Fig.1). It is geographically bounded by 39°46' 47" E and 39°55'40"E longitudes and 8°46'30" N and 9°00'00'N latitudes and occupies an area of about 45km². The site can be accessed by using vehicles. The southern part of the lake is connected to the main highway via several roads all leading to Metahara farms

.A major portion of the study area is dominated by numerous and continuous faulted ridges forming alternate horsts and grabens. The elevation of the lake and its surrounding are between 900 and 1000m above sea level. The lake catchment runs North – East to South – West, bounded in the north by mount Fentale and in the South – East by Dodoti ridge. It runs parallel to the River Awash, but is prevented from draining in to it by an uplifted basaltic ridge. Slopes of the catchment are steepest in the north and west (exceeding 80% on the slopes of mount Fentale) and least on the exposed lacustrine sediments of the valley floor (less than 1% near Abadir farm).

1.1.2 CLIMATE

The middle Awash basin containing the lake is situated in the semi-arid climatic belt in the "Horn of Africa" (Ministry of Water Resources, 1997).

The occurrence of rainfall is strongly influenced by the orientation of topography to the southwest equatorial air stream, which moves northwards with the inter-tropical convergence zone that is the main source of rainfall in the Awash Basin.

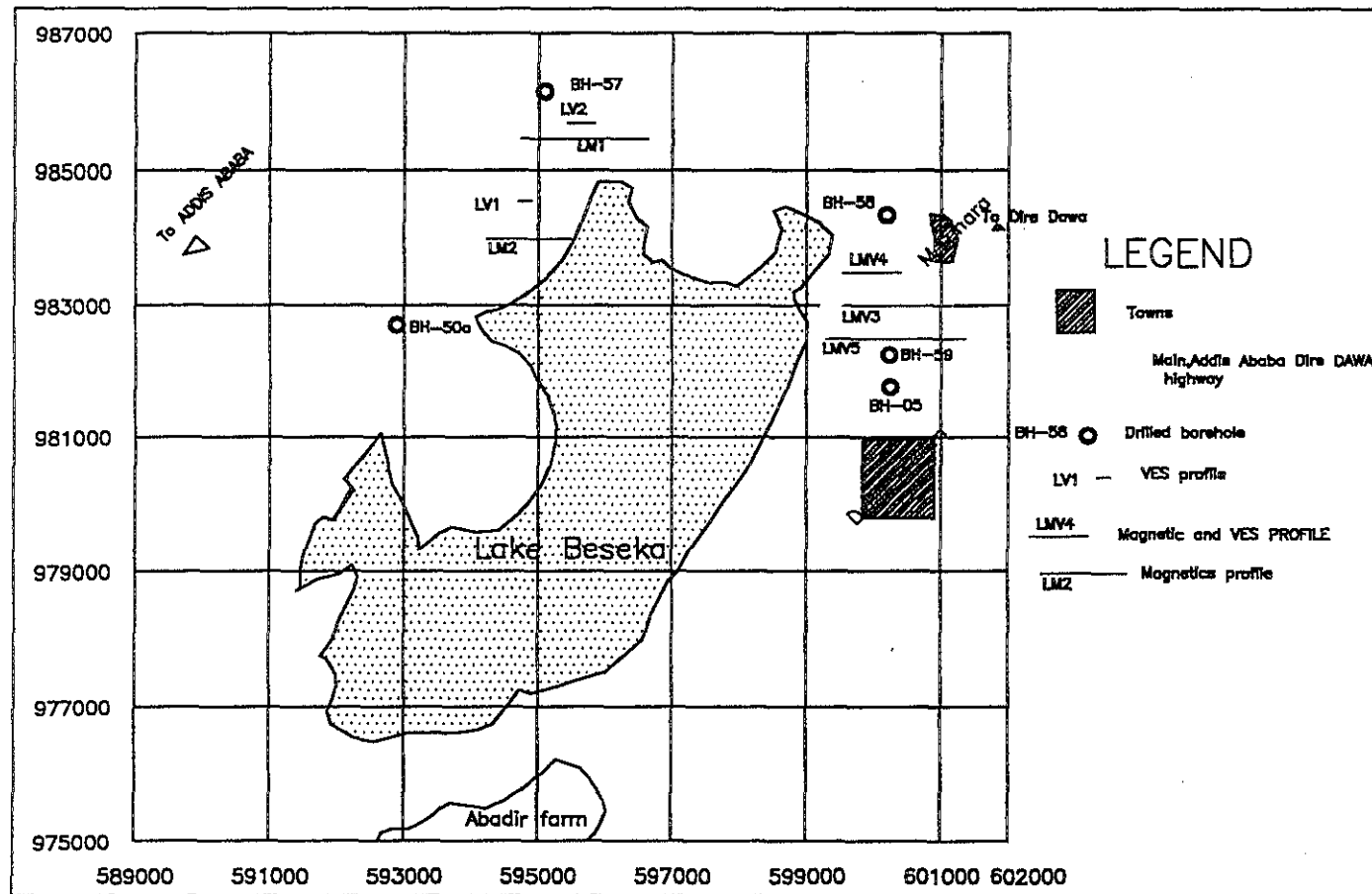


Fig. 1 Location map of the survey area and layout of geophysical lines.

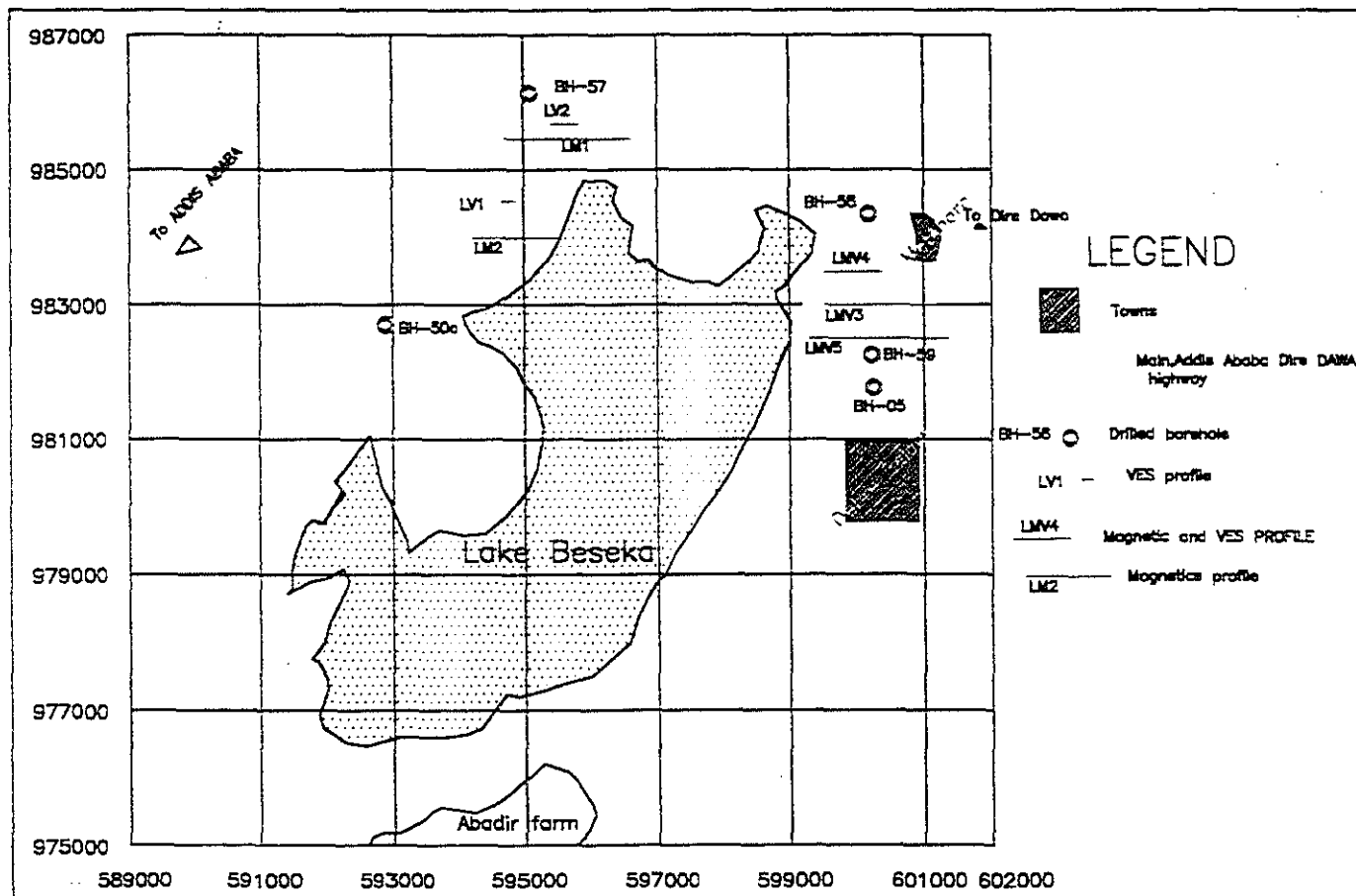


Fig. 1 Location map of the survey area and layout of geophysical lines.

The mean annual rainfall is about 549mm. The mean monthly temperature varies from about 28^oc in June to 21^oc in December. Records of the sunshine hour indicate the actual hours of daily sunshine varieties of hours (June and July) to 9 hours in November and December. The run of the wind in the area varies from 93km/day (November) to 183km/day (July). Measured evaporation data from 45 class pan (EPAN) gives a mean annual class "A" pan evaporation of 2758mm. (Ministry of Water Resources, 1997).

1.2 PREVIOUS GEOPHYSICAL AND GEOLOGICALWORKS

The geological and tectonic activities of the main Ethiopian rift that consists of the study area has been the subject of interest for many years.

Geophysical investigations consisting of seismic refraction, vertical electrical sounding (VES) and magnetic surveys were carried out at selected sites around the lake (E.I.G.S, 1998). The geophysical survey was aimed at obtaining subsurface information that would help in the remedial measures for the Beseka Lake level rise.

According to the technical report (E.I.G.S, 1998), the small volume of geophysical work in a relatively wide area, for the initially stated objectives, has generally become insufficient to get accurate information in outlining structures, mapping zones of hydrologic interest, the water table and specially in indicating groundwater flow direction. The correlation between the geophysical results and available borehole logs was limited.

Considerable changes which have been taking place over the last twenty-three years, have resulted in an increase of the surface area of Lake Beseka from 30km² to about 45² km,

corresponding increase in level from 941m above BND (Blue Nile Datum) to 951m BND since 1976.

This continuously expanding lake is threatening the important lines of communication to the coastal ports and it is also anticipated to bring environmental hazards by flooding the nearby grazing land and irrigation farms and destabilize development activities unless appropriate measures are taken in due time.

To this end, geological, hydrogeological and geophysical studies have been carried out at different times to give remedial measures on the rise of the lake level. Despite that most of the remedial measures recommended especially by Halcrow (1978) were implemented on the unsatisfactory irrigation practices at Abadir farm, the lake level continued increasing constantly. Therefore, a need arose to conduct geophysical surveys around the lake using appropriate methods. In addition to the geophysical surveys carried out by E.I.G.S (19988), supplementary geophysical investigations are conducted for this M.SC research work based on the recommendations of water works and design Enterprise and E.I.G.S. (1988) technical report.

Vertical electrical resistivity (VES) and magnetic methods have been applied to many similar situations to map boundaries between layers having different conductivities, for mapping basement surfaces and groundwater and structural discontinuities like faults which may be weak zones used for geothermal exploration. Hence, these methods are chosen to carry out geophysical investigations for the Lake Beseka level rise adjacent to it on selected sites to obtain additional information for the remedial action to the expansion of the lake in correlation with the previous work.

1.3 OBJECTIVES OF THE PRESENT STUDY

The objectives of the study were:

- Identifying the general characteristics of the subsurface geology .
- Determining the depth to the top of the saturated zone over the selected traverses/sites.
- Delineating fractured zones and probable faults along the selected traverses.
- Mapping the water table and if possible, anticipate the possible groundwater flow

1.4 METHODOLOGY

To achieve the objectives of this study all the available information regarding the geological, hydrogeological and geophysical works in the area were gathered from the concerned governmental agencies and technical reports. This is followed by a field survey to select sites and assess the surface conditions before the actual fieldwork is started. After this, vertical electrical resistivity (VES) and magnetic surveys were carried out along selected sites.

In order to get an information about the geological sequences and the associated resistivity values fourteen vertical electrical sounding (VES) measurements were taken applying Schlumberger electrode configuration along five profile lines (fig.1). In addition to this survey three hundred sixty six magnetic observations were conducted to delineate fractured zones and probable faults along the five selected traverses as shown in figure 1

The following table shows the total volume of work covered in this M. SC research work.

No.	Location	Name of the profile	profile length	Profile direction	Northing	VES points	Magnetic observations
1	NW of the lake-above the main road	M ₁	1883m	E-W	985,459	-	88
		V ₁	4m	E-W	985,677	3	-
2	Below the main road -to the western side of the lake	V ₂	212m	E-W	984,280	2	-
		M ₃	1288m	E-W	984-000	-	47
3	Below the main road to the eastern side of the lake	VM ₁	860m	W-E	983,500	3	44
		VM ₂	1620m	W-E	983,000	3	82
		VM ₃	2080m	W-E	982,500	4	105
	Total	7	7363	-	-	14	366

2. GEOLOGY, TECTONICS AND SEISMIC ACTIVITY

2.1 GEOLOGY

2.1.1 Regional Geology of the Study Area

The study area is part of the Main Ethiopia Rift Valley that extends from Lake Chamo in the South to Yangudi Volcano, near Awash station, in the north (Ministry of Water Resources, 1998). The Western and Eastern Ethiopia plateaus that comprise of Tertiary volcanic rocks bound it. The rifting system generally runs in NNE-SSW direction.

The commencement of the formation of the rifting system dates back to early Tertiary, Upper Eocene, where the initial uplifting of the Afro-Arabian doming took place (Mohr, 1971). This is followed by fissural eruptions of the flood basalt known as trap series volcanic that includes Alaji, Aiba and Termaber basalt. According to Kazmin and Seifer (1978.) and other works, the development of the northern part of the Ethiopian Rift started in Lower Miocene.

Later on, a period of tensional fracturing and faulting with subsidence has resulted in the release of silicic volcanic, the Nazareth Group, and Bofa basalt. The latest volcano-tectonic activity took place during Pleistocene to Recent in the Main Ethiopian Rift and is related to the axial extensional zone, the Wonji Fault Belt. The episode associated with the Wonji Fault Belt resulted in the formation of NNE-SSW trending fault swarms shattering the rift floor and creating rift in rift structure and related volcanism, Wonji Group (Mohr, 1971). The Wonji Group includes all rift volcanic formed after the accumulation of Bofa Basalt. It comprises of Dino Ignimbrite (oldest), pantelleritic centers, sub-recent and recent fissure basalt, hyalocalstics and rhyolite domes. The Wonji Fault Belt has an "en-echelon" arrangement believed to be typical of rift phenomenon (Di Paola; 1970). Several fault zones forming horsts and grabens and displacing the recent lava flows have been marked along pre-existing line of

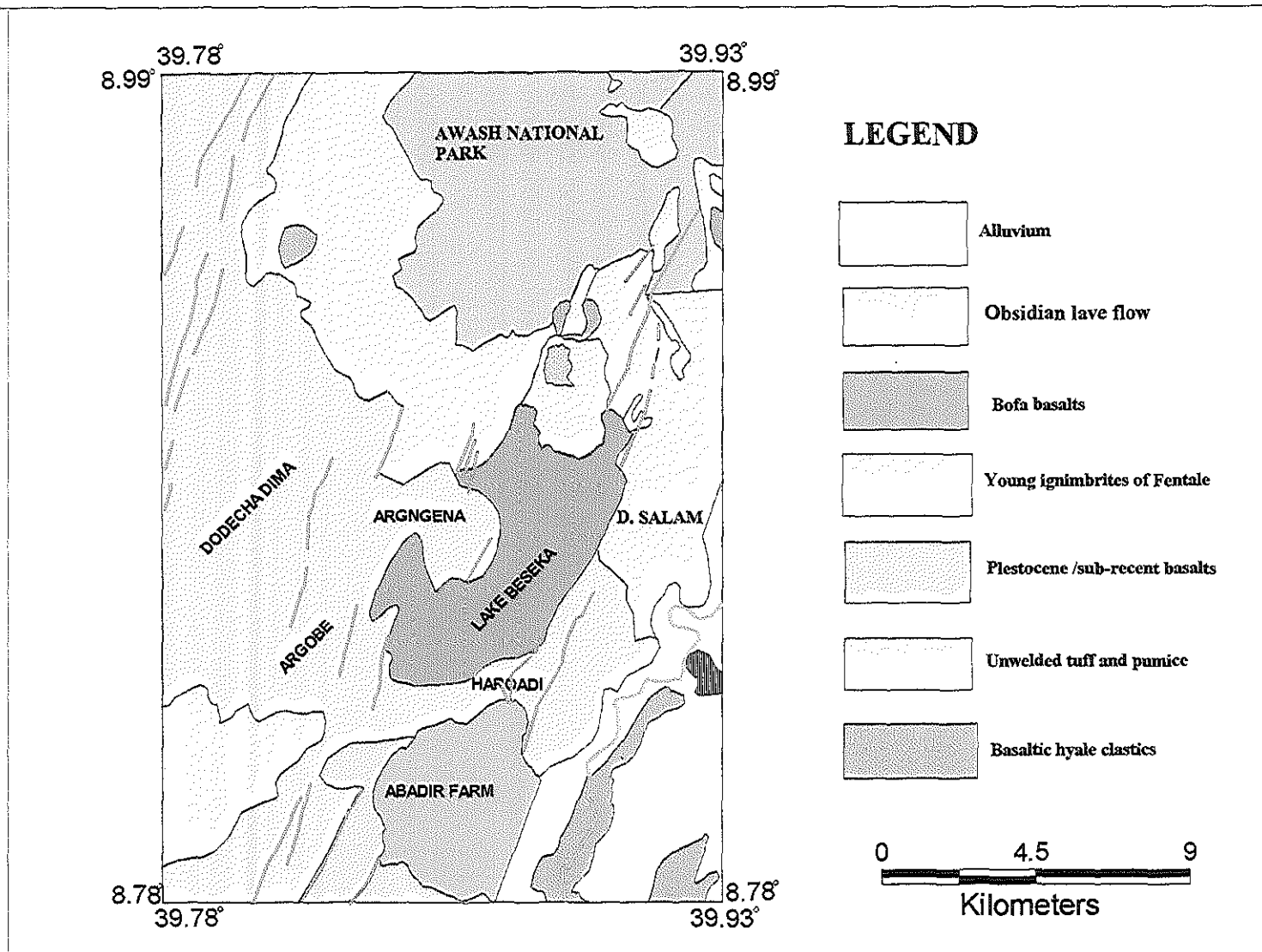
weakness proving rejuvenation of faulting process. The younger faults and fissures post-date the youngest volcanoes.

2.1.2 Local Geology of Lake Beseka and Its Surrounding

The general geology of the area is given in fig. 2. Lake Beseka is part of the large lakes formed during Pleistocene age, in the pluvial periods (Ministry of Water Resources, 1998). The products of Fentale mainly dominate the geology of Lake Beseka area, which is a quaternary strato-volcano. This volcano is predominantly composed of trachytes, rhyolites and pyroclastics of fissural origin associated with the Wonji Fault Belt.

Different stages of volcanic eruptions were observed in this area. The initial stage of the eruption resulted in the release of trachytic lava, which are exposed southeast of Fentale volcano. The activity continued with the effusion of rhyolites, obsidian and interrelated pyroclastics mainly pumice. The final stage of the Fentale volcano was characterized by the eruption of a very extensive welded ash flow tuff, Fentale ignimbrite, which caused the summit caldera to collapse. The ignimbrites for isolated blisters believed to have formed by the presence of steam pockets which bulged the surficial portion of the still hot and plastic material. The steam could have been produced by the sudden vaporization of water from shallow lake or swampy areas beneath the flow at the moment of eruption. Some of the blisters are complete and others are ruptured by secondary steam explosion (Gibson, 1970)

In the northwest of the lake several hyaloclastite cones and tuff rings are identified. The hyaloclastites are results of a sudden contact of basaltic magma with cold water or saturated sediment.



9

Fig.2 Geological Map of Lake Beseka (adopted from the report of EIGS,1998).

The northern portion of the lake is covered by "aa" basalt flow which has erupted between 1810 and 1839 (Ministry of Water Resources,1998) through 94km. long fissure system.

“Pleistocene to sub-recent Basalts” underly much of the surrounding area of the lake; often fairly coarse grained with phenocryst. These rocks are exposed in most of the fault scarps near the perimeter of the lake. In addition to basalts, superficial deposits are found to exist (alluvial clays and silts) that occupy Metahara and Abadir farms and also lacustrine deposits cover part of the lake surrounding.

2.2 TECTONIC FEATURES UNDERLYING LAKE BESEKA AND IT'S SURROUNDING

The main structural features of the Ethiopian region are tensional fractures followed by normal and / or reverse faults. All the previous works related to rift tectonics agree on causes of tensional fractures on the present main Ethiopian rift to be up doming terminated by down warping of pre-rift crust due to upper mantle plumbing. Local grabens and horsts have been identified on the recent rocks within the rift indicating the present active tectonic sinking.

Lake Beseka, situated within the axial portion of the main Ethiopian rift valley in the central part of Metahara sub-sheet immediately south of Fentale Volcano, is one of the presently growing lakes along the active rift tectonic axial zone. There is about 5-6 km. wide local graben that is elongated in NE-SW direction in the central part of Metahara sub-sheet south of Fentale pyroclastic Volcano, where Lake Beseka is situated. It is developed on highly fissured and fractured narrow belt of vesicular and aphyric basalt. The fissures and fractures are the manifestation of tensional faults in the area. Towards north, the lake is advancing to cover wide scoraceous zone on the southern part of Fentale pyroclastic Volcano. The lake is

also spreading in NE-SW direction within the graben. Fault escarpments are observed on both sides of the lake. Eastern and Western Beseka Lake fault planes (escarpments) face each other and have high dip angles. These prominent fault escarpments are found affecting the ignimbrite on both sides of the lake. The northern part of the lake lies over the recent aphyric basalt and young ignimbrite of Fentale within the deeply space northeast and northwest faults/fractures. The central part of the graben that is occupied by Lake Beseka is found to be maximum axial depression of the Fentale region.

The open fissures along this zone have NNE-SSW and frequently observed at immediate northwest, northeast and southwest of Beseka Lake. Some of the open fissures trending along NE-SW are more than 1km. long with an average opening of 2 meters wide. Example of such prominent fractures is observed at a locality called Enkufutu, immediate northwest of Beseka Lake. Similar prominent open fractures with similar trend are observed at a locality known as Tony where there are six hot springs vigorously discharging hot water to the lake. All the hot springs in the region are associated with such deep—rooted structures.

The northern continuity of this structure is submerged under the lake along which the Chaleletu and other already covered hot springs were located. Some of these deep-rooted open fractures are commonly associated with NW-SE and E-W trending, densely spaced fractures. To the north of the Fentale pyroclastic cone, a local graben which may be the northern continuity of the southern graben within which Lake Beseka is found, is identified and mapped (Ministry of Water Resources, 1998). This northern extension of the Beseka graben has been affected by recent tectonic movement which resulted in deep fractures and faulting similar to the southern graben (Di Paola, 1970) There are also hot springs manifestation mentioned by the locals and some of them are found by the Ministry of water

Resources personnel. The overall situation seems to indicate that the Beseka Lake is more affected by such zonally concentrated structures.

2.3 EFFECTS OF SEISMIC ACTIVITY ON BESEKA

LAKE LEVEL RISE

The seismic activity in the northern sector of the main Ethiopian Rift has been in significant in the previous 20 years of instrumental recording until the occurrence of the 1981 earthquake swarm in the rift axial zone around the area between the quaternary silicic Volcanic center of Fentale and Dofan (Asfaw L.M., 1981). This earthquake swarm started in mid-January and lasted until early March with some of the earthquakes having maximum local magnitude of 4.4. The maximum energy released corresponds to the location of Awara Melka where new surface fractures were also formed.

A major earthquake swarm with a local magnitude of 4.7 also affected the vicinity of Fentale in 1989 (Ministry of Water Resources, 1998). The rift floor between Fentale Volcanic center and Nazareth town is relatively quite in seismic activity as revealed by the absence of instrumental recording or reports. In this sector, the western rift escarpment region and the adjacent plateau have been more active than the rift floor.

As a whole the seismic data clearly show the occurrence of the present day Volcano-tectonic activity which manifests itself in the rejuvenation of existing faults, fractures and fissures and the development of similar new features.

It may be worth while to consider the possible effect the earthquake activity may have had on the rise of Beseka Lake since 1978. The effects of earthquakes include violent ground motion

accompanied by surface rupture and displacement. Secondary effects include a variety of events such as liquefaction, regional subsidence or emergence of landmasses. Effects of this deformation may result in regional changes in ground water levels. In many earthquakes there have been accounts of water being forced out of the ground during or after the events. Observations have also been made in which others had an increased flow. The result of seismic activity is, however, an increase in the amount of groundwater released.

The above discussion may suggest that the Beseka Lake level rise may have been enhanced as a result of the 1981 and 1989 earthquake swarms. The volcanic activity could have reactivated existing faults, fractures and fissures and generated new ones at depth in the vicinity of Beseka, as observed on the surface at Awara Melka. It is reasonable to suggest that the groundwater system in this region was affected by the seismic activity with a net result of increasing the amount of groundwater released to the lake itself.

The earthquakes occurred on the western rift escarpment and adjacent plateau are associated with normal faults with minor strike-slip components. The faults and fractures formed as a result of these events constitute more favorable regional conditions for the percolation and recharge of surface water into the groundwater system finally raising the overall groundwater level in the rift axial zone.

The seismic activity at the axial zone of the rift has revealed active volcanic activity that may be associated with the ascent of magma beneath the quaternary silicic volcanoes as well as active tectonic activity that may be associated with rift extension and separation. The volcanic and tectonic episodes strongly imply that severe thinning of the crust is occurring beneath the Fentale-Beseka area consistent with the overall evolution of the rift itself.

3. THE ELECTRICAL RESISTIVITY METHOD: BASIC THEORY AND MATHEMATICAL FOUNDATIONS

3.1 INTRODUCTION

The aim of applied geophysics is to deduce the physical properties of the earth and its internal constitution from the physical phenomena associated with it. Geophysical methods are widely employed in detecting and mapping underground inhomogeneities and structures, which are not available from surface geological observations. It provides the tools for solving various geological problems particularly in the field of applied geology and engineering (Dobrin

Electrical resistivity methods are the most widely used techniques of geoelectric exploration, which have been successfully applied in the study of different geological and hydrogeological problems and groundwater exploration by utilizing the electrical properties of rocks. The electrical conductivity of earth material can be investigated by introducing a current (DC or AC) into the ground using two or more electrodes, and the potential is measured between two points (probes) suitably chosen with respect to the current electrodes.

Electrical resistivity methods are used to obtain structural and lithological information such as, the location of fault and shear zones that could affect the pattern of groundwater flow, the location of groundwater table, etc. In this work, the variation of resistivity with depth is studied by a progressive increase of current electrode with a method known as vertical electrical sounding (VES). This method provides an adequate depth of penetration and quantitative result without the large cost involved in an extensive drilling program (Kearey *et al.*, 1984).

The subsurface rock resistivity variation affects or perturb the electrical current flow lines and these in turn affect the distribution of surface electrical potential lines, compared to their pattern over a homogeneous medium. The computed quantity is known as the apparent resistivity (ρ_a). Therefore, from the measurement of potential/potential gradients on the surface it is possible to know something about the nature of the subsurface layers.

3.2 EARTH RESISTIVITY

3.2.1 Basic Idea and Scope

In the electrical resistivity method a direct commutated or low-frequency alternating current is introduced in to the ground by means of two electrodes (metal stakes or suitably laid out bare wire) connected to the terminals of a portable source of e.m.f (Parasnis D.s., 1986). The resulting potential distribution on the ground, mapped by means of two probes (metal stakes or, preferably, non-polarizable electrodes), is capable of yielding information about the distribution of electric resistivity below the surface of the earth.

3.2.2 Current Flow and Potential Distribution over a Homogeneous Earth

It is necessary to find the relation for the flow of current in the ground and distribution of potentials at the surface to get the fundamental equation of the electrical resistivity method in order to determine the resistivity of the earth.

Considering a continuous current flowing in an isotropic homogeneous medium, the current density J is related to the electric field intensity E by Ohm's law:

$$J = \frac{1}{\rho} \vec{E} = \sigma \vec{E} \quad (3.1)$$

The electric field is the gradient of a scalar potential,

$$E = -\nabla V = -gradV \quad (3.2)$$

Thus, eqn. (3.1) can be expressed as:

$$J = -\frac{1}{\rho} \nabla V = -\frac{1}{\rho} gradV = -\sigma V \quad (3.3)$$

where, ρ is the resistivity of the medium

σ is the conductivity of the medium

V is the conductivity

The flow of current in a medium is expressed based on the principle of conservation of charge

as:

$$divJ = -\frac{\partial q}{\partial t} \quad (3.4)$$

where J is the current density

q is the charge density

For a stationary/direct current and eqn. (3.4) reduces to:

$$divJ = 0 \quad (3.5)$$

$$div\left(\frac{1}{\rho} gradV\right) = 0 \quad (3.6)$$

Substituting eqn. (3.3) in eqn. (3.5) we get.

$$grad\left(\frac{1}{\rho}\right) gradV + \frac{1}{\rho} divgradV = 0 \quad (3.7)$$

This is the fundamental equation of electrical prospecting with direct current. For a homogeneous medium, p is constant. As a result of this the first term of eqn (3.7) vanishes and it reduces to:

$$\nabla^2 V = 0 \quad (3.8)$$

Thus, the electrical potential distribution for direct current in a homogeneous isotropic medium satisfies Laplace equation.

3.2.3 A Point Source of Current Over a Semi-Infinite Homogeneous Medium

When a current I is introduced into the semi-infinite homogeneous and isotropic earth in the downward direction at a point P_1 , the potential at a distance r from P_1 will be only a function of r and Laplace equation can be written as:

$$\frac{d^2 V}{dr^2} + \frac{2}{r} \frac{dV}{dr} = 0 \quad (3.9)$$

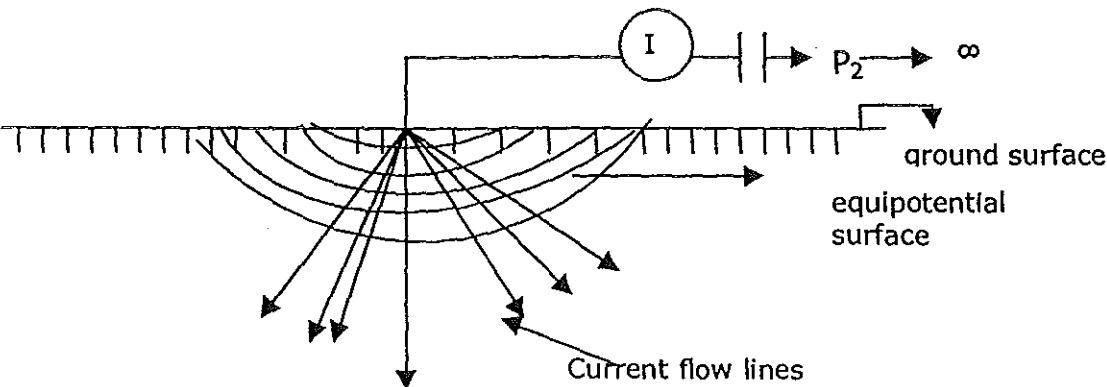


Fig. 3. Distribution of current in a semi-infinite medium due to a point source of current.

The current circuit as shown in the figure is completed through another electrode placed at infinity where its influence is negligible. Multiplying by "r" and integrating from r to ∞ the solution of eqn (3.9) is

$$V = \frac{A}{r} + B \quad (3.10)$$

$$J = \frac{-1}{\rho} \frac{dV}{dr} = \frac{1}{\rho} \frac{A}{r^2} \quad (3.11)$$

As the potential is taken to be zero at a large distance ($r \rightarrow \infty$) from the source, the integration constant B=0. Then, the current density J at a distance "r" is given by:

The total current flowing out of a hemispherical surface of radius "r" is given by the relation:

$$\begin{aligned} I &= 2 \Pi r^2 J = 2 \Pi r^2 \left(\frac{A}{\rho r^2} \right) \\ &\Rightarrow I = 2 \Pi \frac{A}{\rho} \\ &\Rightarrow A = \frac{I \rho}{2 \Pi} \end{aligned}$$

Thus, the potential at any point due to a current source at the surface of a homogeneous earth is:

$$V = \frac{I \rho}{2 \Pi r} \quad (3.12)$$

From this relation ,

$$\rho = 2 \pi r \frac{V}{I} \quad (3.13)$$

3.2.4 Two Sources of Current Over a Semi-Infinite Medium

In practice, the current is introduced into the ground by means of two electrodes (a source and a sink) as shown in the figure below:

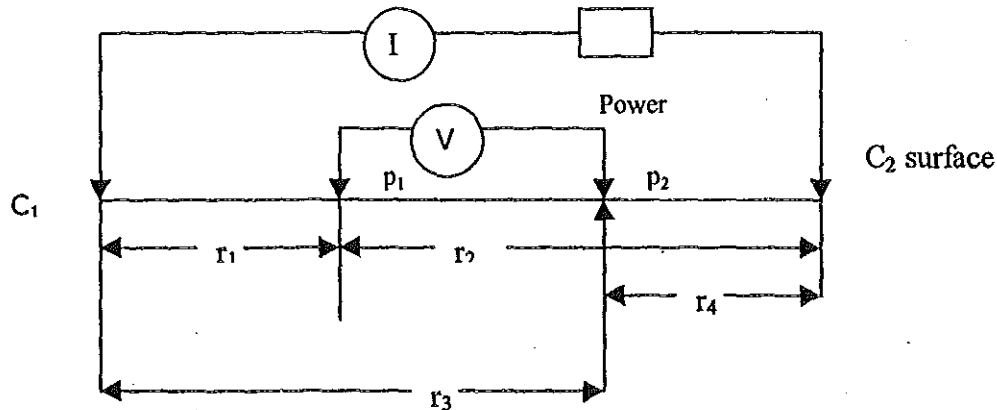


Fig. 4. The current and two potential electrodes on the surface of a homogenous isotropic ground of resistivity ρ .

When the distance between the two current electrodes is finite, the potential at any nearby surface point will be affected by both current electrodes. As eqn. (3.12) the potential due to C_1 at P_1 is

$$V_1 = \frac{-A_1}{r_1},$$

$$\text{where } A_1 = -\frac{I\rho}{2\Pi} \Rightarrow V_1 = \frac{I\rho}{2\Pi} \left(\frac{1}{r_1} \right)$$

Because the currents at the two electrodes are equal and opposite in direction, the potential due to C_2 at P_1 is

$$\Rightarrow V_2 = \frac{-I\rho}{2\Pi} \left(\frac{1}{r_2} \right)$$

$$V_2 = \frac{-A_2}{r_2},$$

$$\text{where } A_2 = \frac{I\rho}{2\Pi} = -A_1$$

Thus the total potential at P₁ is given by

$$V_{P_2} = V_1 + V_2 = \frac{I\rho}{2\Pi} \left(\frac{1}{r_1} - \frac{1}{r_2} \right) \quad (3.14)$$

Similarly the total potential at P₂ will be

$$V_{P_2} = \frac{I\rho}{2\Pi} \left(\frac{1}{r_3} - \frac{1}{r_4} \right) \quad (3.15)$$

Finally, the potential difference ΔV between the inner potential electrodes P₁ and P₂ is given

by:

$$\nabla V = V_{P_1} - V_{P_2} = \frac{I\rho}{2\Pi} \left[\left(\frac{1}{r_1} - \frac{1}{r_2} \right) - \left(\frac{1}{r_3} - \frac{1}{r_4} \right) \right] \quad (3.16)$$

Therefore
$$\rho = \frac{2 \Pi V}{I} \left[\left(\frac{1}{r_1} - \frac{1}{r_2} \right) - \left(\frac{1}{r_3} - \frac{2}{r_4} \right) \right] \quad (3.17)$$

Or,
$$\rho = k \left(\frac{\nabla V}{I} \right)$$

Where,
$$K = 2 \Pi \left[\left(\frac{1}{r_2} - \frac{1}{r_2} \right) - \left(\frac{1}{r_3} - \frac{1}{r_4} \right) \right]^{-1}$$

, is the geometric factor of configuration

3.3 APPARENT RESISTIVITY

In a homogeneous ground, a single measurement of the current and potential difference would determine its resistivity. Therefore, the resistivity derived in eqn. (3.17) is constant for any current and electrode arrangement.

If the ground is inhomogeneous, however, and the electrode spacing is varied, or the spacing remains fixed while the whole array is moved, the measured potentials will change. As a result of this condition the resistivity varies for each measurement. This measured quantity, which is intimately related to the arrangement of electrodes is known as the apparent resistivity. Although it is diagnostic, to some extent, of the actual resistivity of a zone in the vicinity of the electrode array, the apparent resistivity is definitely not an average value and only in the case of homogeneous grounds is it equal to the actual resistivity. However, apparent resistivity can be calculated using eqn. (3.17) for any electrode configuration.

4. INSTRUMENTATION, ELECTRODE LAYOUTS AND FIELD PROCEDURE, INTERPRETATION, DATA PROCESSING AND PRESENTATION

4.1 INSTRUMENTS USED FOR VERTICAL ELECTRICAL SOUNDING

(VES) SURVEY

All vertical electrical sounding (VES) data measurements were made using PASI-16GL earth resistivity meter and PASI-P300 energizer, electrodes, cables and reels for measuring current and voltage.

The 16 GL earth resistivity meter can carry out and memorize acquisitions with a resolution of 16 bit. The instrument is based on a multiprocessor system that can autonomously generate the energetic wave-by means of the input of a current by two electrodes AB-and contemporaneously acquire data to the measuring electrodes MN. The data is treated internally in floating-point format. The first field measurement starts with the NEW SESSION. If the Y button is pushed, it is possible to alter the value of the acquisition parameters. On the other hand, the parameters are not displayed and the wave will be created with pre-set values when the N button is pushed. Finally the message "WAIT" will appear during which the acquisitions takes place. At the end of the measurement the voltage (potential difference), the current, their ratio and the progressive numbers of the acquisition are displayed simultaneously. The voltage value is free of the spontaneous potential, dynamically deducted at every cycle.

The instrument is completely controlled and programmed by a keyboard with four buttons integrated on the frontal panel. For a good functioning of the keyboard, the buttons should be

pressed in a resolute and non-persistent way. Each time a button is pressed the instrument makes a sound. The anti-pressure valve under the handle is used to restore the internal pressure of the instrument. After a flight or an ascension in height, it results impossible to open the cover this valve must always stay locked (screwed down) and may only be opened for a short period if it is not possible to open the watertight cover.

The instrument is equipped with an AUTORANGING system, which automatically adjusts the acquisition scale on the grounds of the selected parameter. Before starting the programmed acquisition, one, two, or three test acquisitions are carried out in order to determine the best reading scale (for this reason, the preset cycles can be preceded by one, two, or three cycles). Each acquisition proceeded by two readings corresponding to the positive semiwave and two readings corresponding to the negative semiwave, both for the voltage and current.

The energizer can work with an internal or external battery. But, an internal battery is used turning the power switch to ON INT position. The power can be regulated according to the needs keeping the stand by switch to off position.

4.2 ELECTRODE LAYOUTS AND FIELD PROCEDURES

The variation of electric conductivity with depth is explored by vertical electrical sounding (VES) field procedures using the symmetrical Schlumberger array electrode configuration. In this configuration electrodes are arranged symmetrically in the sequence AMNB, the current electrodes on the outside and the potential electrodes on the inside along the line to be surveyed as shown in the figure below.

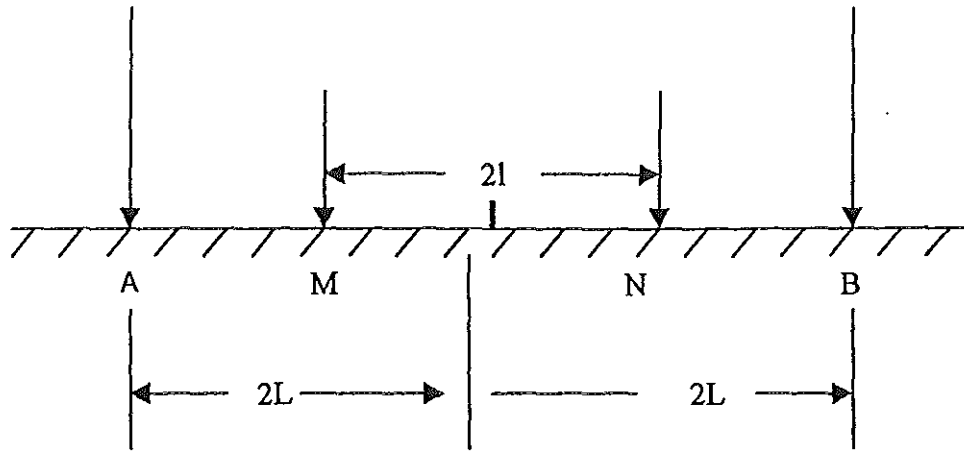


Fig. 5. The Schlumberger electrode configuration

Because the fraction of total current that flows at depth varies with the current electrode separation, the field procedure is to use a fixed center with an expanding spread. The potential electrodes were kept fixed and the current electrodes were moved outward after every measurement to change the depth range of the measurements. At some stage the potential dropped below the reading accuracy of the resistivity meter in which case the distance between the potential electrodes was increased three times progressively up to 90m. Repeated measurements were taken at 40m, 60m, 300m and 440m separations of AB at the old and new distances of MN. The maximum range of separation (AB) used between the current electrodes was 1000m.

The sounding data were taken at intervals of 260m from west to east along four profiles below the main road and east of the lake. The distance between any two of these profiles is 500m. The sounding data for the rest two profiles located in the northwest of the lake were collected at 200 and 260 m intervals from west to east. The sites were selected based on the stated objectives and surface conditions.

The apparent resistivity values were obtained by multiplying the geometrical factor K with the integrated values ($\Delta V/I$) read from the instrument. After this the data points were immediately

plotted on a double log-log paper and decisions were made whether to repeat the measurement or not from the qualitative nature of the field curve by visual inspection

4.3 INTERPRETATION OF VERTICAL ELECTRICAL SOUNDING DATA

There are two types of vertical electrical sounding (VES) interpretation, direct and indirect interpretation methods. The direct method provides procedures for obtaining the layer parameters directly from the apparent resistivity measurements (Slichter, 1933). The indirect method comprises curve matching between the vertical electrical sounding (VES) curves obtained from the field and the curves computed for assumed theoretical models, the auxiliary point method, automatic forward and inversion methods.

4.3.1 Curve Matching by Master Curves

This method involves a comparison of the measured curve with a set of theoretically calculated master curves. The theoretical master curves are plotted resistivity versus electrode separation on a logarithmic graph paper with modules of 62.5 mm. There are many albums of theoretical curves computed using different techniques. Some of them are Mooney and Wtzed (1956) computed using numerical integration. Orelana and Mooney (1966) use the image point computation method. Computation by decomposition into partial fractions was used to produce the collection of the companies Generale de Geophysique (1955). This technique is practicable only when the number of layers is small, say up to four. Even for four-layer case the number of reasonable parameter combination is so large and the collection of curves is so bulky that interpretation by matching become impractical. Therefore for a large number of layers it is virtually impossible. Currently this type of curve matching is obsolete.

4.3.2 Partial Curve Matching

This technique requires matching of small segments of the profile with theoretical curves (master curves and auxiliary curves) for two or if possible, three horizontal layers. Generally one would start from the left-hand (small spacing) side of the curve and match successive segments towards the right (large spacing). When the portion of the field curve is reasonably matched in this way all the layers in this segment are lumped together and assumed to have an effective resistivity ρ and depth Z_e . This lumped layer is used as a surface layer and the next portion of the field curve is interpreted in a similar way. Here we discuss the two layer partial curve matching. This method requires two layer master curve and four auxiliary curves for curve types H, Q, A and K. The interpretation procedures are:-

1. Trace the field curve on a transparent paper which is scaled the same as the master curve.
2. Match the left hand portion of the field curve to a master curve. From this match, trace the origin of the master curve (first cross) which designates (h_1, ρ_1) and the ratio of ρ_2/ρ_1
3. Superimpose the transparent paper on the auxiliary curve of the right type. Keep axes parallel at all times (on master curve and auxiliary curves). For Q and H type curves, place the first cross over the coordinate origin of the auxiliary. For A and K type curves, place the first cross over the left-hand vertical axis of the auxiliary curve, corresponding to the value of ρ_2/ρ_1 .
4. Select the curve on the auxiliary curves, which corresponds to ρ_2/ρ_1 and trace this curve on the transparent paper starting from the first cross.
5. Superimpose the transparent paper on the master curve again, now to fit the next part of the field curve by sliding the transparent paper on the origin of the master curve along the auxiliary curve previously drawn

6. On the transparent paper mark the position of the second cross and the resistivity ratio which fits the second part of the field curve on the master curve sheet. The resistivity ratio gives $\mu = \rho_3 / \rho_e$. The second cross gives (h_e, ρ_e)
7. Super impose the field curve again on the auxiliary curve, place the first cross on the same position as step 3. The position of the second cross lies on a dashed line which gives $v = h_2 / h_1$
8. In the same way the above procedure will continue until the whole field curve is completely matched.

4.4 DATA PROCESSING AND PRESENTATION

The observed apparent resistivity curve plotted against half current electrode separation ($AB/2$) on a double logarithmic paper of modules 62.5 mm. at every VES point is segmented and can't be interpreted as it is. In order to get reliable information from the curve the effect of the displacement of the segment, which is attributed due to the change in the geometry of the configuration and in homogeneity of resistivities near the potential electrodes was corrected. Approximate interpretation method (auxiliary point method) was initially applied on the raw data for the determination of layer resistivity and thickness. As in the other potential field investigations, resistivity survey in particular vertical electrical sounding (VES) is subjected to equivalence problem. To solve this problem, direct iterative interpretation methods of curve generation and fitting procedures were applied.

The layer parameters, resistivity and thickness, obtained by iteration processes were used to construct geoelectric sections for each profile (Figs. 7,8,10,12 and14) to show the direction of different lithologic units in vertical direction. Apparent resistivity pseudosections were prepared by gridding and contouring the raw resistivity data corresponding to different depth

levels obtained at each VES stations along the profiles to assess the vertical resistivity variation qualitatively.

5. BASIC THEORY AND FIELD SURVEY OF THE MAGNETIC METHOD

5.1 INTRODUCTION

The magnetic method of prospecting is one of the oldest geophysical methods, which was applied to locate iron-ore deposits for the first time as early as 1640 (Sweden). Like gravitational methods in contrast to electrical and seismic methods, it utilizes a natural field of force consisting of the field of geologic bodies and the terrestrial magnetic field. Contrary to their gravitational attraction (which exists independently of the earth's field), the magnetic responses of geologic bodies frequently depend on the direction and magnitude of the earth's magnetic field. The law controlling the magnetic attraction (Coulomb's law) is identical in form with that governing gravitational attraction. Hence, magnetic interpretation problems may often be handled by a simple adaptation of the relations, which apply in gravitational work.

Magnetics is generally more complex and variations in the magnetic field are more erratic and localized due to the time dependence, the variable direction and the difference between the dipolar magnetic field and the monopolar gravity field. Magnetic field variations are often diagnostic of local as well as regional structures such as faults, and it is the most versatile of geophysical techniques. However, because of the spontaneous nature of subsurface effects, it is not possible to control the depth of penetration in magnetic prospecting.

The magnetic fields of geological bodies, which manifest themselves as disturbances in the normal geomagnetic field (magnetic anomalies), are present because these contain various amounts of ferromagnetic minerals and they were formed and are situated within the earth's magnetic field. The configuration of the anomalies is affected by the shape, dimensions, position, depth, petrography, etc. of the associated geological inhomogeneities (Telford W.M.,

1990). Anomalies can be determined from field observations and analysed by interpretational procedures, from which an important information can be obtained. Anomalies cannot be observed directly; the absolute or relative total geomagnetic field or of its components are observed and the anomalies are then determined from them as regional or local irregularities.

5.2 FUNDAMENTAL PRINCIPLES OF THE MAGNETIC METHOD

The magnetic method consists of measuring the magnetic field of the earth as influenced by rock formations having different magnetic properties and configurations. The measured field is the vector sum of induced and remanent magnetic effects. Thus, there are three factors, excluding geometrical factors, which determine the magnetic field. These are the strength of the earth's magnetic field, the magnetic susceptibilities of the rocks present and their remanent magnetism. The earth's magnetic field is similar in form to that of a bar magnet. The flux lines of the geomagnetic field are vertical at the north and south magnetic poles where the strength is approximately 60,000n. In the equatorial region, the field is horizontal and its strength is approximately 30,000nT.

The primary geomagnetic field was applied for the purpose of mineral exploration surveys, constant in space and time. Magnetic field measurements may, however, vary considerably due to short-term external magnetic influences and the magnitude of these variations is unpredictable. Therefore, it is necessary to take continuous readings of geomagnetic field with a base station magnetometer while the magnetic survey is being done.

The intensity of magnetization induced in rocks by the geomagnetic field F is given by

$$I=KF \quad (5.1)$$

Where, I is the induced magnetization

K is the volume of magnetic susceptibility, and
F is the strength of the geomagnetic field.

For most materials, K is very much less than one. If K is negative, the body is said to be diamagnetic. If K is a small negative value, the body is said to be paramagnetic. If K is a large positive value, the body is strongly magnetic and it said to be ferromagnetic.

The susceptibilities of rocks are determined primarily by their magnetic content since these minerals are so strongly magnetic and so widely distributed in various rock types.

The remanent magnetization of rocks depends both on their composition and their previous history; where as the induced magnetization is nearly always parallel to the direction of the geomagnetic field and the natural remanent magnetization may bear no relation to the present direction and intensity of the earth's field. The remanent magnetization is related to the direction of the earth's field at the time the rocks were last magnetized. Movement of the body through folding etc. and the chemical history since the previous magnetization are additional factors, which affect the magnitude and direction of the remanent magnetic vector.

Thus, the resultant magnetization M of a rock is given by:

$$M = M_n + KF \quad (5.2)$$

where M_n is the natural remanent magnetisation, and F is a vector which can be completely specified its horizontal(H) and vertical(Z) components and by the declination(D) from true north.

5.3 EARTH'S MAGNETIC FIELD

5.3.1 Elements of the Earth's Magnetic Field

At every point along the earth's surface, a magnetic needle free to orient itself in any direction around a pivot at its centre will assume a position in space determined by the direction of the earth's magnetic field F at that point. Hence, the earth's magnetic (geomagnetic) field vector F at any point P above the earth's surface is parallel to the line of force passing through this point and its magnitude and direction is are functions of p . Since measuring instruments conventionally installed in magnetic observatories respond only to the horizontal component H of the actual field, it is customary to resolve the vector F in to x , y and the vertical component z . The vector H that lies on xy -plane determines the direction of the magnetic meridian at point p . The angle between the geographic and magnetic meridians is the magnetic declination; if the magnetic meridian is to the east of geographic, the declination is east (positive), if it is to the west, the declination is negative. The angle between the horizontal plane and the vector is the magnetic inclination (dip) I ; if F points below the horizontal plane, the inclination is positive; if it points above the horizontal plane, it is negative.

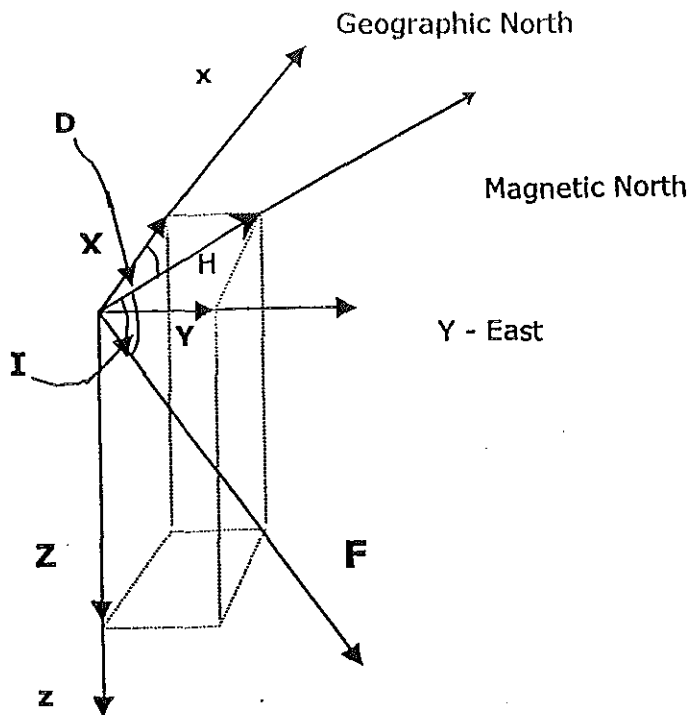


Figure 6. Elements of the Earth's magnetic field

The quantities X, Y, Z, D, I, H AND F, known as the magnetic elements, are related as follows:

$$H = F \cos (I)$$

$$Z = F \sin (I) = H \tan (I)$$

$$X = H \cos (D)$$

$$Y = H \sin (D) \tag{5.3}$$

$$X^2 + Y^2 = H^2$$

$$F^2 = H^2 + Z^2 = X^2 + Y^2 + Z^2$$

5.3.2 Origin of the Geomagnetic (Total) Field (B_d)

The total magnetic field shows irregularities at different points on the surface of the earth. These irregularities are detected by the small variations of a compass reading or magnetometer at different points on the surface of the earth. In order to identify the anomalies in the earth's field it is clearly essential to know its undisturbed character.

As far as exploration geophysics is concerned, the geomagnetic field of the earth is composed of three parts:

5.3.2.1 The Main Field

To a very close approximation the main geomagnetic field can be represented formally as the field of a point dipole situated almost at the center of the earth with its magnetic moment pointing towards the earth's geographical south. This field originates from the magnetic field of the dipole field and magnetism of magnetized crustal material or rock magnetism. The magnetic field of the dipole is the strongest part of the total magnetic field generated by the fluid outer core. It is 99percent of the total magnetic field. This secular part or the dipole field is a large, slowly changing part of the field (almost static) caused by the internal state of the earth and is mathematically described by the International Geomagnetic Reference Field (IGRF). IGRF(s) are series (updates) of mathematical models, which describe the main geomagnetic field and its secular variations. It causes the total magnetic field to reverse its polarity over along geologic time known as polarity reversal. The total magnetic has not always had its present (normal) polarity with the north magnetic pole close to the north geographic pole and the south magnetic pole close to the south geographic pole over geologic history total magnetic field has intermittently reversed in polarity. Thus there have been times in geologic past when the north magnetic pole has been located close to the south geographic pole and the south magnetic pole has been located close to the north geographic pole and in such situations the field is said to be reversed.

5.3.2.2 The External Magnetic Field (B_{sw})

The external magnetic field originates from magnetic field induced by the flow of ionized particles (ions) emitted by the sun within the ionosphere towards the magnetic poles. They

result from a solar wind, a constant stream of ionized particles emitted from the sun. It accounts about 0.5 percent of the total field. They are related to support activity and causes diurnal variation in the total field known as the magnetic storm. The diurnal part is a relatively small and erratically changing part of the magnetic field, which repeats cyclically. This field is monitored by measuring the magnetic field at a single or multiple (tied) station(s) situated in magnetically quiet areas. This measurement is made at short and regular time intervals, synchronous with field survey.

5.3.2.3 Local Magnetic Anomalies (Rock Magnetism)

This part of the field is the magnetic field caused by lateral magnetic susceptibility inhomogeneities in the subsurface. It originates from magnetized crustal rocks associated with geologic structures. It is variable and the weakest of the other field. Under certain circumstances rocks record (retain) the earth's past magnetic field. This recorded rock magnetism either increases or decreases the total magnetic field observed today by magnetic measurements giving rise to either positive or negative magnetic anomalies. Therefore, facts enabled geophysicists to estimate dates and past positions of the plate tectonics from magnetic measurements and confirm the idea of sea-floor spreading. This part is of chief interest in magnetic prospecting / mapping. The secular or diurnal parts must be evaluated and removed (normal and diurnal variations) in order to obtain the anomalous part. The anomalous part, which is obtained after normal and diurnal corrections, is considered to represent a picture of all departures from a horizontally homogeneous magnetization in the earth's crust and may be interpreted qualitatively and/or quantitatively in terms of the lithology and structure (Nettelton, 1940).

The magnetic anomaly is given by:

$$\Delta B = B_{\text{obs}} - B_D - B_{\text{SW}} \quad (5.4)$$

5.4 INSTRUMENTATION AND FIELD PROCEDURE

Scintrex made proton precision magnetometer (IGS-MP-3/4) was used for the magnetic survey. This magnetometer has three mode of operations: total field, gradiometer and the base station. Among these modes the total field was selected for this survey. The automatic tuning feature with a tuning field of 35,000nT was selected and readings were taken at 20m station intervals.

To take the most accurate magnetic measurements, the sensor was properly aligned within the sensor holder, which is attached to the back harness provided. All magnetic objects such as belt buckles, pens, knives etc., which affect magnetic readings were removed away during surveying.

Moreover, one base station was established and diurnal variations were monitored. Readings were taken on this base station before and after conducting magnetic survey along each line to make a diurnal correction.

5.5 INTERPRETATION OF MAGNETIC DATA

Interpretation of magnetic data is quite often qualitative because of the erratic and complex character of magnetic maps or profiles. The diurnal corrections are performed accurately for each magnetic observations using the formula:

$$Y_{\text{corr}} = Y_{\text{obs}} + Y_{\text{ref}} - Y_{\text{base}} \quad (5.5)$$

$$Y_{\text{base}} = (Y_1 + (\Delta Y / \Delta t)(t - t_1)) \quad (5.6)$$

Where Y_{corr} —is corrected value

Y_{obs} —observed value

Y_{ref} — the average base station reading

Y_1 – base station reading at time t_1

Y_2 base station reading at time t_2

$$\Delta_Y = Y_2 - Y_1$$

$$\Delta_t = t_2 - t_1$$

t – time during observation

In addition to this, a moving window averaging program with number of stations ($n = 3$) has been used to remove noisy observations. Finally, this corrected data is processed by using Oasis Montaj V.4.3 software to produce the end result of the magnetic survey (profiles and contour maps).

Indeed the technique is something a fine art; the interpreter in magnetics can usually see geological structure merely by looking at magnetic map, much as one can visualize surface features from the contours of a topographic map.

GEOPHYSICAL RESULTS

6.1 VERTICAL ELECTRICAL SOUNDING (VES) RESULTS

The geoelectric sections obtained from the vertical electrical sounding surveys along the five profiles are given in Figures 7 to 12. The interpretations of these sections are as given below.

6.1.1 PROFILE ONE

Profile one consists of two VES points. Along this profile four major layers have been discerned from the interpretation of sounding curves (Fig. 7). The top layer is characterized by a resistivity range of 6-8 Ohm-m with almost uniform thickness of 1.5 m and 1.6 m. Taking into account visual field observations and the nearby borehole information these resistivity values are attributed to silt sand that covers the upper part of the lithologic succession.

The second layer in this geoelectric stratum is relatively resistive ranging from 32-33 Ohm-m. The thicknesses of the layer are 22m and 16.9m around the vicinity of VES 1.1 and VES 1.2 respectively. This formation could be related with hard welded tuff.

The third layer of this profile is highly conductive with uniform resistivities of 2.6 Ohm-m and 2.5 Ohm-m probably due to the intrusion of the lake water (saline). But the thickness of this section is variable, which is about 36.9 m around VES 1.1 and 85.7 m around VES 1.2. As to the groundwater condition of the area, it seems favorable for accumulating subsurface water. Hence, the resistivity response of this layer is an indication of water saturation and it could correspond to welded tuff. Based on this result the average depth of the water bearing horizon from the surface is about 24 m.

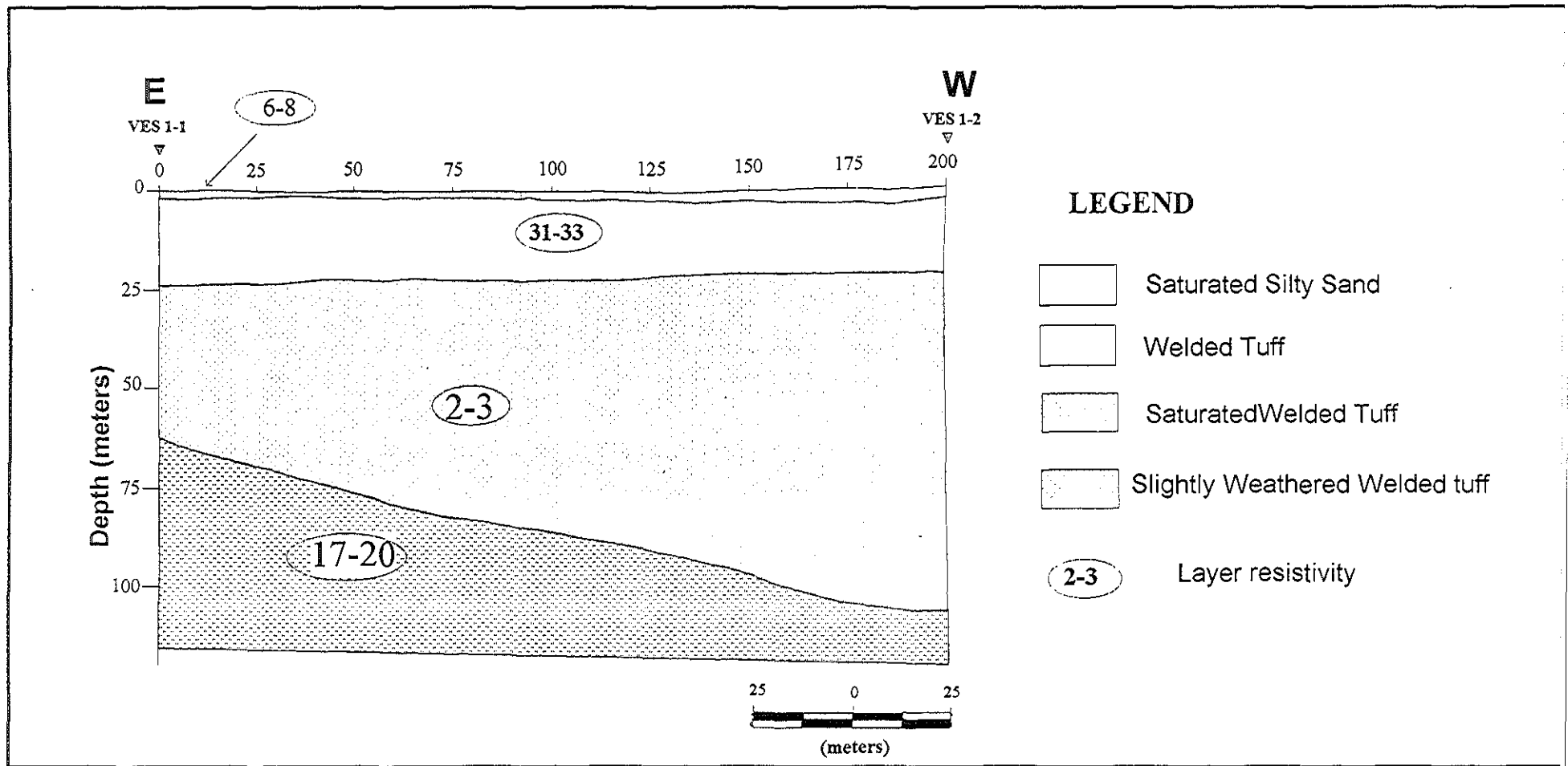


Fig. 7 Geoelectric section along line LV1 (NW of Lake Beseka)

The layer underlying the conductive zone, which represents the bottom section, has intermediate resistivities of 20.2 Ohm-m and 17.2 Ohm-m at VES 1.1 and VES 1.2 respectively. The formation of this relatively impermeable layer may correspond to a slightly weathered welded tuff.

6.1.2 PROFILE TWO

The result of vertical electrical sounding (VES) survey conducted along this profile has revealed (Fig. 8) that the apparent resistivity curves are found to represent a model having five geoelectric layers. The geoelectric layers consisting the top most part of the layer are characterized by minimum thickness 0.8-1.6m and high resistivity ranging from 239 to 577 Ohm-m. Taking into account the borehole information (BH 57) available in the area, those high resistivity values are attributed to dry silty sand that cover the upper part of the lithologic succession.

The second layer in the sequence has extremely variable resistivity values around each VES station. The formation resistivity value (117.2 Ohm-m) around VES 2.1 could be attributed to less saturated silt sand. The resistivity value (26.2 Ohm-m) around VES 2.2 may correspond to a moderately water saturated silty sand. The high resistivity value (529.7 Ohm-m) in the vicinity of VES 2.3 is assumed to have a similar resistivity formation but it may be relatively dry.

The third layer; which is distinguished by a resistivity range of 39 to 66 Ohm-m appears to represent the same lithology. The thickness of this layer varies from 48 to 60 m, where the

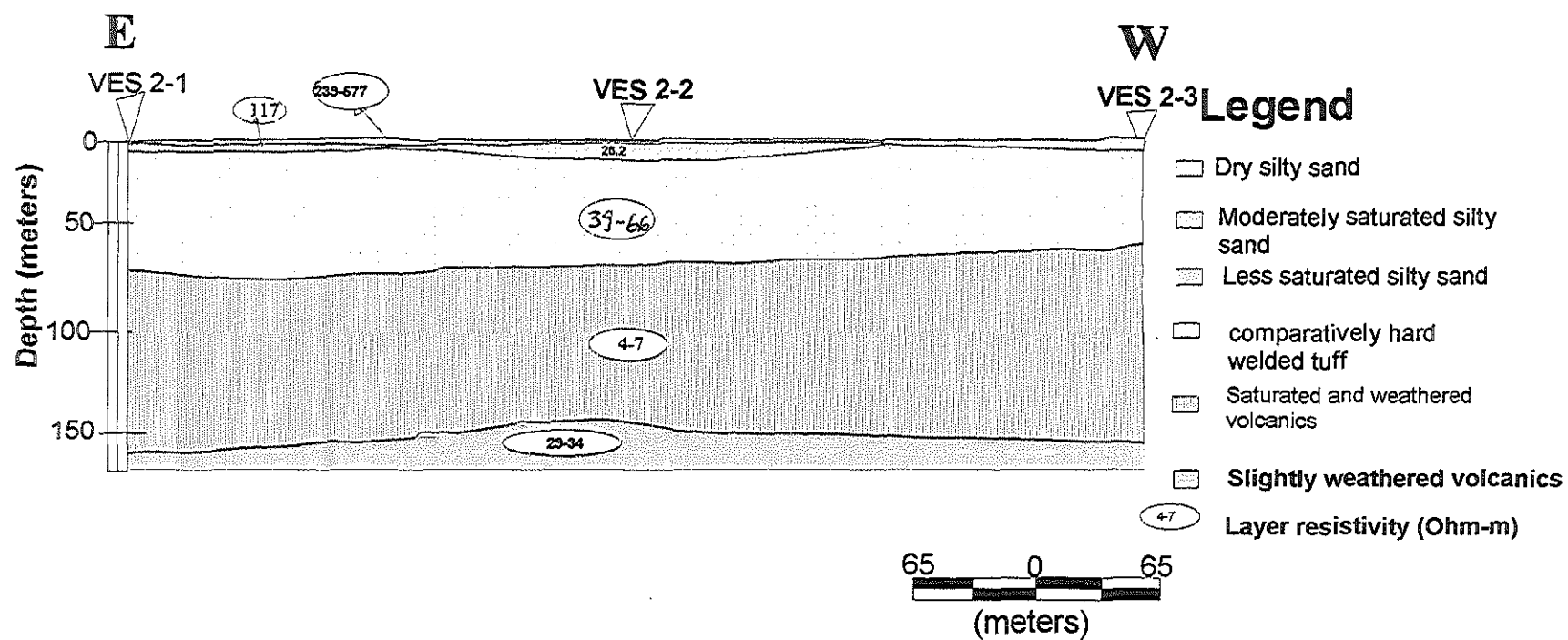


Fig. 8 Geoelectric section along line LV2 (NW of Lake Beseka)

maximum thickness (60m) is attained in the vicinity of VES 2.2. Lithologically, this layer is interpreted has comparatively fresh and hard welded tuff.

The fourth and relatively thick horizon shows low resistivity response, in the range from 4 to 7 Ohm-m, with a thickness variation of 86 to 102 m This section appears to be highly saturated with saline water. Lithologically, it could be attributed to weathered volcanics (tuff). The average depth to the water table from the surface is estimated to be about 60 m. The underlying layer beneath the saturated zone is represented by a relatively high resistivity ranging from 29 to 34 Ohm-m, which may be classified as slightly weathered volcanic (tuff).

As shown on the corresponding apparent resistivity pseudosection (fig. 9) very high resistivity formations are found to exist at the top layer in the vicinity of VES 2.1 and VES 2.3 terminated by a relatively low resistivity formation around VES 2.2. This lateral resistivity variation at the top layer may be due the effect of weathering and sedimentation. The lateral resistivity variation beneath the top layer appears to be decreasing depthwise

6.1.3 PROFILE THREE

The overall picture of the geoelectric section along profile three (Fig.10) indicates that the resistivity of the top layer lacks uniformity and the thickness of each layer increases from VES 3.1 to VES 3.3. The possible explanation for the distortion around the vicinity of VES 3.1 and VES 3.2 is that the water table is found at shallow depth near to the lake.

The resistivity response around VES 3.1 of the top layer is low probably due to the intrusion of the saline lake waters or weathering. However, it is described weathered welded tuff

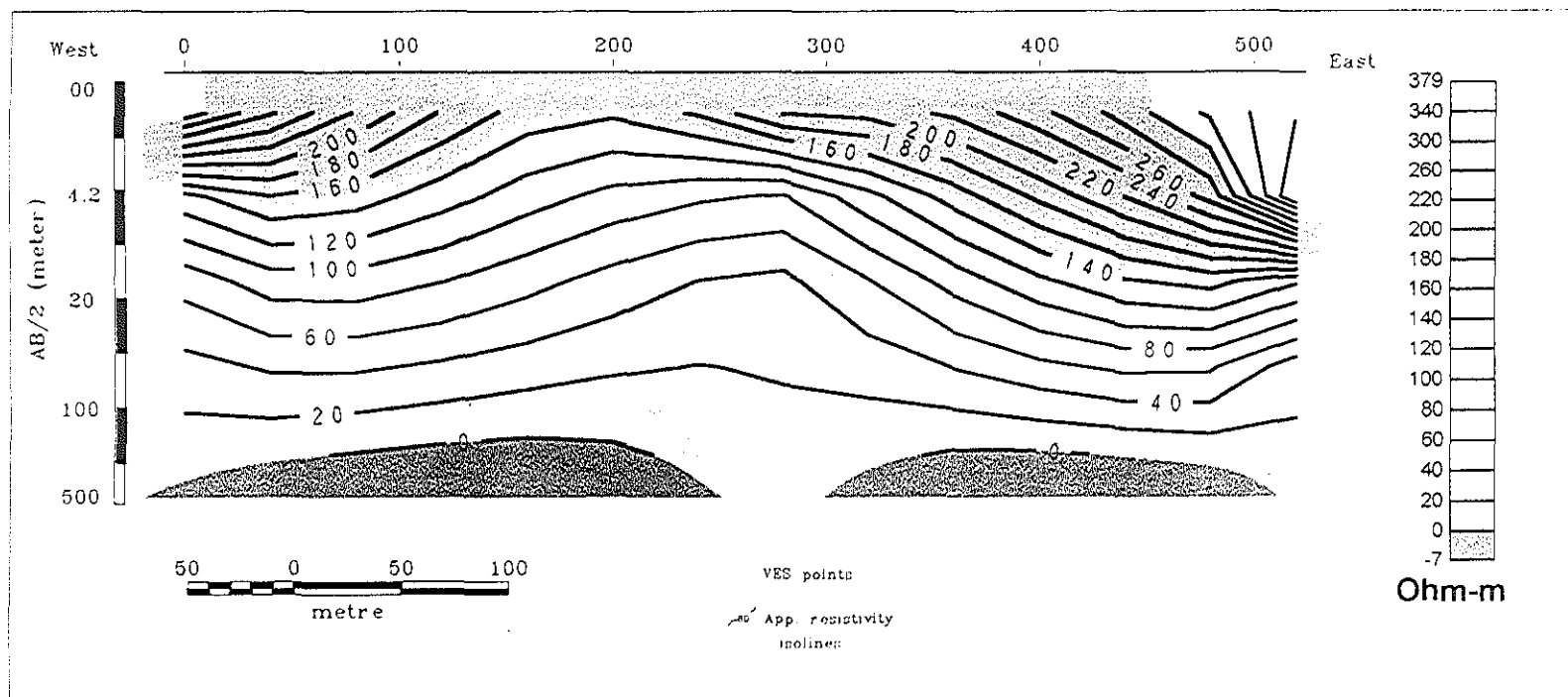


Fig. 9 Apparent Resistivity Pseudosection along Line LV2, east of Beseka
June. 2001

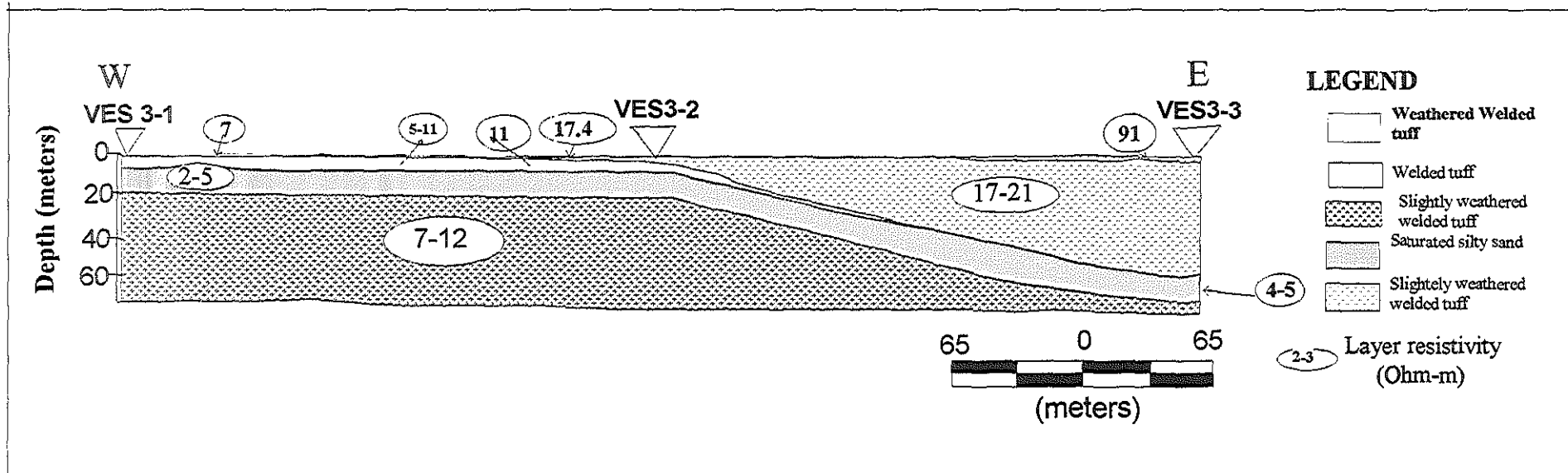


Fig. 10 Geoelectric section along line LMV3 (NE of Lake Beseka)

lithologically. The highest resistivity value (91 Ohm-m) of the top layer in the vicinity of VES 3.3 with a thickness of 1.6 m may correspond to welded tuff.

The top most layer in the vicinity of VES 3.2 and the second layer around VES 3.3 ranging from 17 - 22 Ohm-m is lithologically characterized as slightly weathered volcanics (welded tuff). However, the layer around VES 3.3 is extending to a depth of about 56 m that may also consists of silty sand formation.

The resistivity value in the vicinity of VES 3.1 and VES 3.2 underlying the top layer is varying in the range of 5-11 Ohm-m with almost uniform thickness of 4.7 m and 3.8 m respectively. These low resistivity values are obtained probably due to moisture content or salinity of the formation. Thus, this section can be described generally as saturated welded tuff.

The third layer constitutes the water bearing horizon (saturated zone). This section exhibits very low resistivity values ranging from 2-5 Ohm-m a thickness variation of 2-14m. The low resistivity values along this profile are the signature of the intrusion of the lake water into this saturated zone. From the nearby borehole information in the area this layer can be attributed to be saturated silt sand. The depth of the water table around VES 3.1 and VES 3.2 is about 5m and it extends to about 58m around VES 3.3.

The bottom layer underlying the saturated horizon is a less saturated aquifer with a resistivity range of 7-12 Ohm-m in comparison with the overlying layer. This layer can be interpreted as slightly weathered saturated welded tuff.

The apparent resistivity pseudosection (Figure 11) along profile 3 shows that the resistivity contour lines distribution exhibits a gradual increasing trend towards the top layer. The top part of this layer is dominated by high resistivity values around VES 3.1 and VES 3.3. The saturated zone underlying the moderately resistive horizon in this pseudosection is uplifted in the vicinity of VES 3.1 and VES 3.2 as it is shown on the geoelectric section (Fig. 11).

6.1.4 PROFILE FOUR

Three soundings, VES 4.1, VES 4.2 and VES 4.3 were taken along this profile at station intervals of 260m. From the interpretation of vertical electrical sounding (VES) survey conducted along profile four (Fig.12) four different resistivity layers have been identified. The top most layer shows a resistivity variation from 13 Ohm-m to 143 Ohm-m. The relatively thin (0.9m) and lower resistivity (13.1 Ohm-m) horizon, which was mapped in the vicinity of VES 4.2 may correspond to weathered welded tuff. The higher resistivity values (104 - 143 Ohm-m) whose thickness are 1 m and 1.6 m around VES 4.1 and VES 4.3 respectively, could possibly attributed to welded tuff.

The second layer in the sequence mapped persistently along this profile has a resistivity range between 37 and 57 Ohm-m. The thickness of this layer, which varies from 3-36 m is considerably thick around VES 4.3 and it is lithologically classified as moderately weathered welded tuff.

The resistivity response of the third layer that exhibits uniform resistivity values ranging from 5 - 6 Ohm-m is the zone of interest from hydrogeological point of view. The thickness of the layer, which varies from 14 to 46m increases progressively from VES 4.1 to VES 4.3. Based on these results, the likely depth to the water table in the area would be at about 5m. Thus this layer is interpreted as water saturated horizon consisting of probably completely weathered

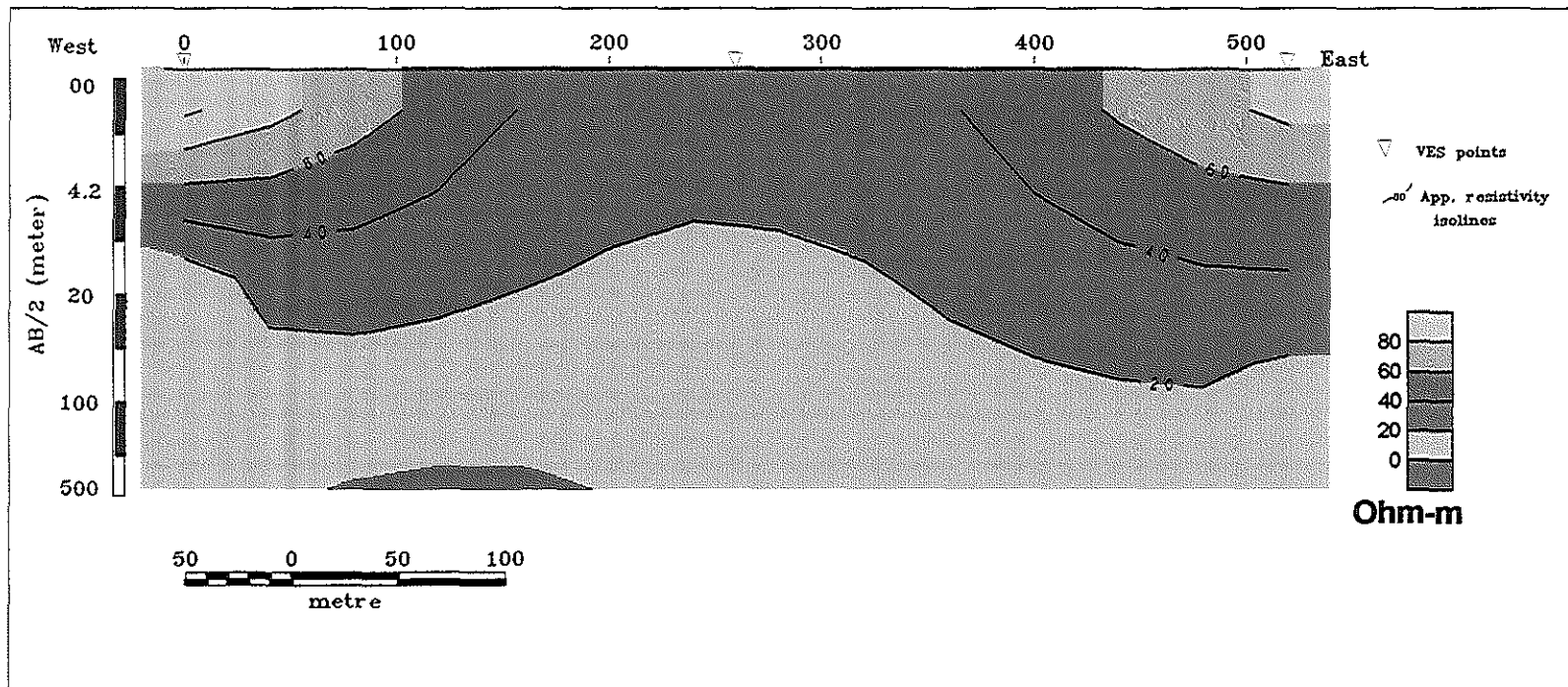


Fig.11 A pparent Resistivity Pseudosection along Line LMV3, east of Beseka
June, 2001

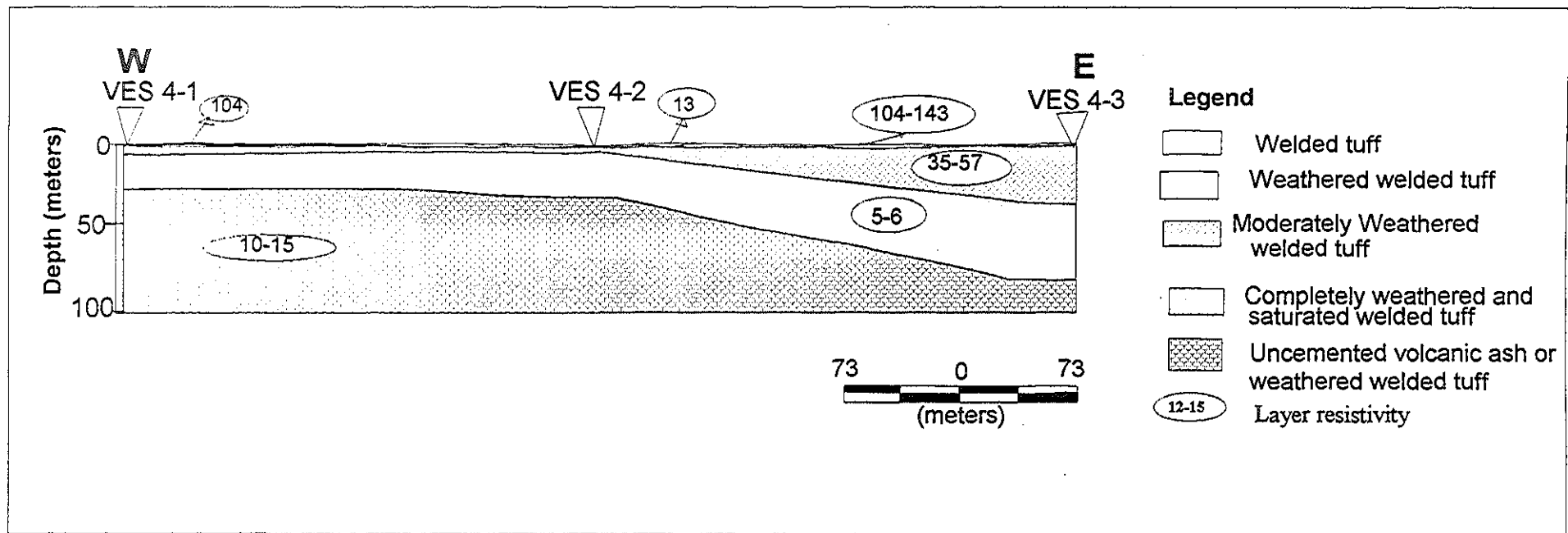


Fig.12 Goelectric section along line LMV4 (NE of lake Beseka)

Welded tuff, which is considered to be the favorable lithological unit for accumulating fluids in their pore spaces.

The bottom geoelectric layer underlying the saturated zone is represented by the resistivity response varying from 10 - 15 Ohm-m. These values indicate that the layer may not be an aquiclude and could form part of the aquifer with moderate permeability and porosity. This formation could be composed of uncemented volcanic ash or weathered welded tuff. The slight increase in resistivity values with respect to the overlying layer could be explained by the vertical variation in the permeability of the lithologic units. Based on the description of borehole BH-58 the lithology in the area is a sequence of tuffaceous rock of various texture.

The apparent resistivity pseudosection along line LMV₄ (Fig.13) clearly shows the low resistivity formation (saturated) extending diagonally starting from the top layer in the vicinity of VES 4.1 to the bottom of the last VES point. From this we can understand that the aquifer systems are highly saturated in the vicinity of the lake due to the intrusion of the saline lake water. As it is interpreted in the geoelectric section (fig. 12) a high resistivity formation is also seen at the top of the layer in the vicinity of VES 4.3 demarcated by a moderately resistive formation. The overall resistivity picture of this pseudosection shows that the resistivity of the formations increase away from the lake.

6.1.5 PROFILE FIVE

The geoelectric section (Fig. 14) consisting of four layers is constructed from the interpreted data of three sounding stations. The top resistivity layer ranging from 3.6 to 4.5 Ohm-m around VES 5.1 and VES 5.2 with an average thickness of 1.5m may be associated with highly weathered welded tuff. This low resistivity range might be also obtained due to the salt

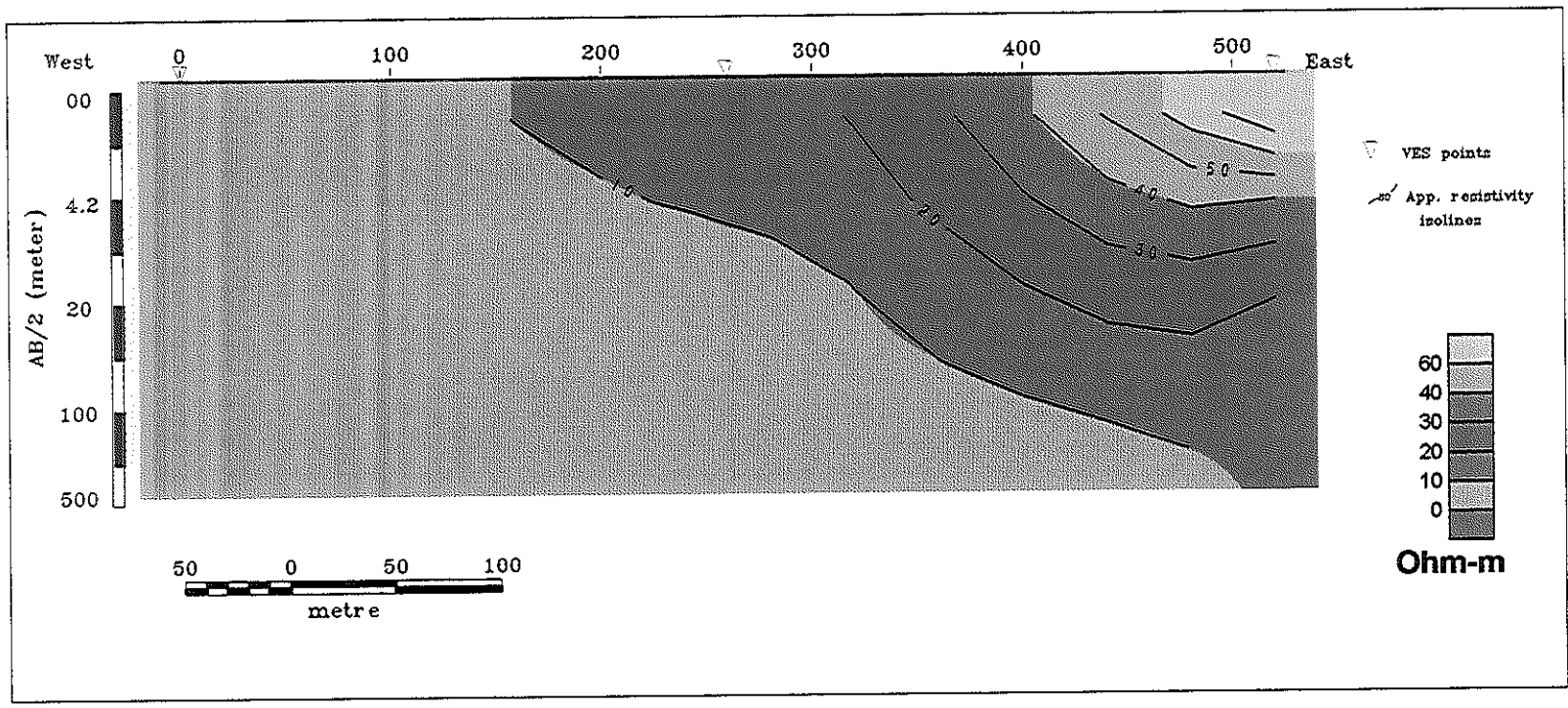


Fig. 13 Apparent Resistivity Pseudosection along Line LMV4, east of Beseka June. 2001

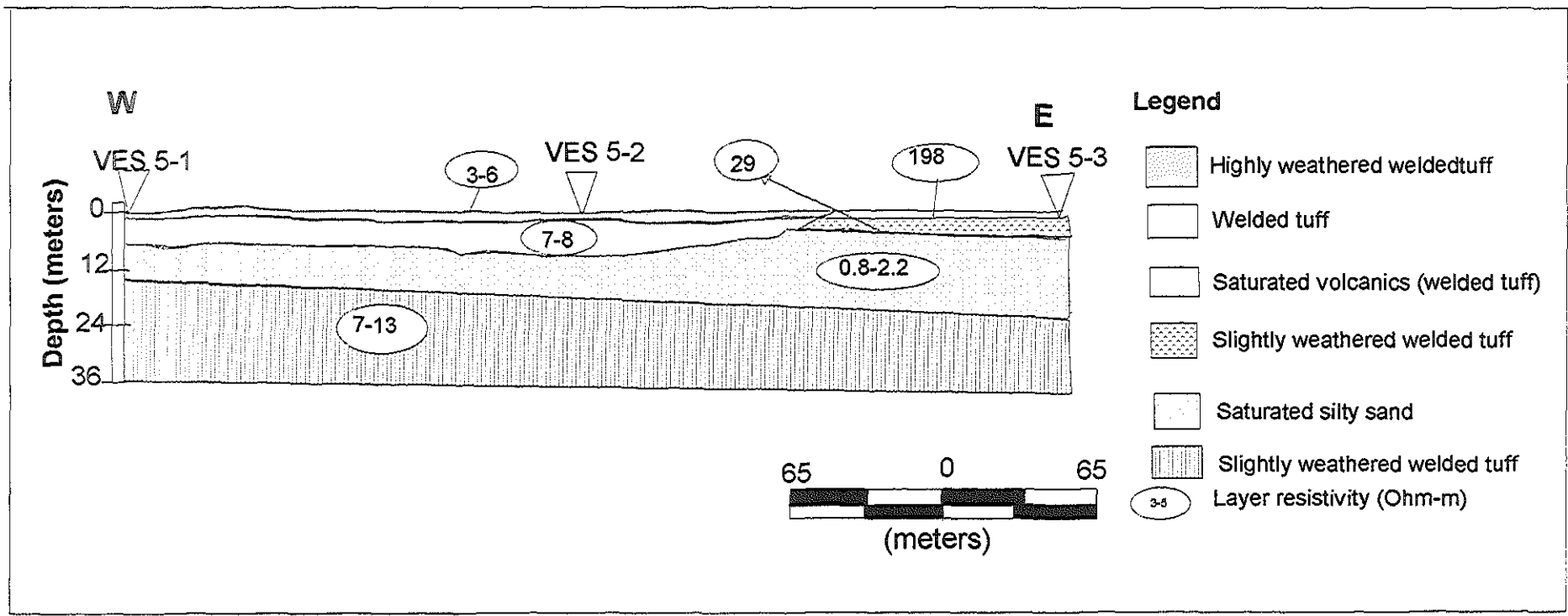


Fig. 14 Geoelectric section along line LMV4 (NE of Lake Beseka)

Content of the formation. The peculiar high resistivity value (198 Ohm-m) with a small thickness of 0.6m around VES 5.3 in the top layer of this profile could be associated with greenish welded tuff according to the borehole (BH 59) information available in the area.

The second layer marked by an average resistivity of 7 Ohm-m in the vicinity of VES 5.1 and VES 5.2 has a thickness variation of 5 to 7m. This low resistivity formation may correspond to saturated volcanics (welded tuff). On the other hand, the resistivity of this section, which has a thickness of 4.7m increases to 29.1 Ohm-m in the neighborhood of VES 5.3. Lithologically, it may be described as slightly weathered weld tuff.

The saturated zone (water bearing horizon) of the third layer has a resistivity ranging from 1 to 2 Ohm-m. These extremely low resistivity values may be caused due to the intrusion of the lake water since the profile is near to the lake. Thus, this layer can be classified as saturated silty sand. The thickness of the layer varies from 8 to 12m and the depth of the water table from the surface is estimated to be about 16m.

The bottom layer, which has a resistivity ranging from 7 - 13 Ohm-m may be revealed with slightly weathered welded tuff. Though this layer shows moderate resistivity values it forms most likely part of the aquifer. The relatively high resistivity values with respect to the overlying layer could be explained by the vertical variation in the permeability (saturation) of the lithologic succession.

This apparent resistivity pseudosection (Fig. 15) is generally characterized by a high resistive formation around VES 5.3 underlain by a relatively low resistive formation as shown in figure 14.

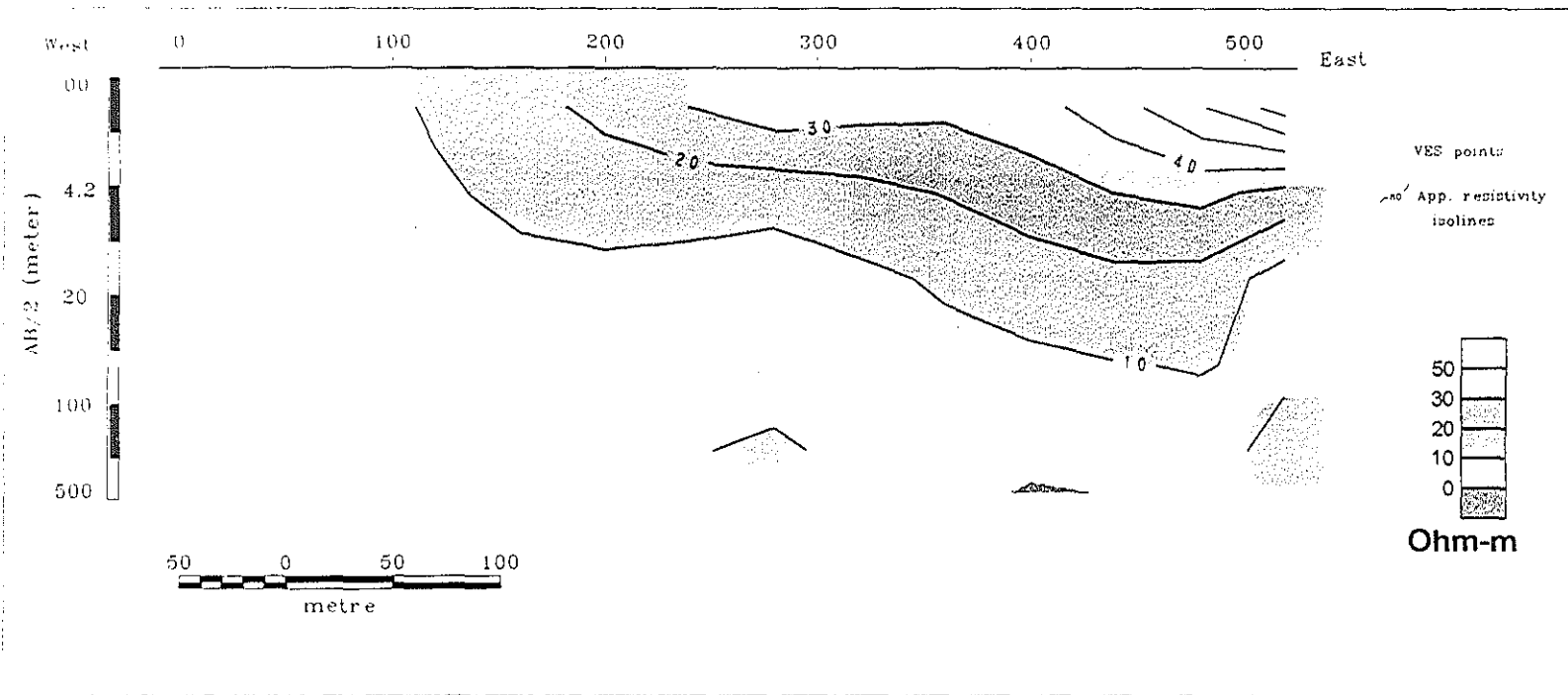


Fig. 15 Apparent Resistivity Pseudosection along Line LMV5, east of Beseka
June. 2001

6.2 MAGNETIC RESULTS

The magnetic profile along line LM₁ (fig.16) is dominated by high frequency magnetic anomalies, which could be associated with the outcrop of volcanic rocks. From the general pattern of this profile, the low magnetic values seen along the traverse may represent fractured formation due to weathering.

The magnetic intensity along line LM₂ (fig.17) is magnetically quite between stations 0 and 200, which shows almost uniform magnetic susceptibility of volcanic rocks. On the other hand, the variation of magnetic intensity with small amplitudes indicates that the magnetic susceptibility of volcanic rocks may vary within short distances. The abrupt magnetic intensity variation at station 600 could be related with the presence of structures (fault/contact).

The magnetic susceptibility of rocks along line LMV₄ (fig.18 (a)) generally shows no significant magnetic variation (disturbance) since the rocks are not exposed to the surface. However, the high magnetic picks observed at the beginning and end of the profile may be related with the exposed welded tuff or near surface rocks as delineated by the vertical electrical sounding survey (VES).

The magnetic profile as observed in fig.18 (b) is marked by various magnetic picks that are associated with surface volcanics or the location of the volcanic at shallow depth, where it is covered by soil. The magnetic values indicating low magnetic susceptibility observed around the end of the profile are assumed to be associated with different geologic structures (fault/shear zones).

As observed in line LMV₅ (fig.19(c)), the area between stations 0 and 750 is magnetically quite, which reflects weathered and highly fractured rocks as detected by vertical electrical

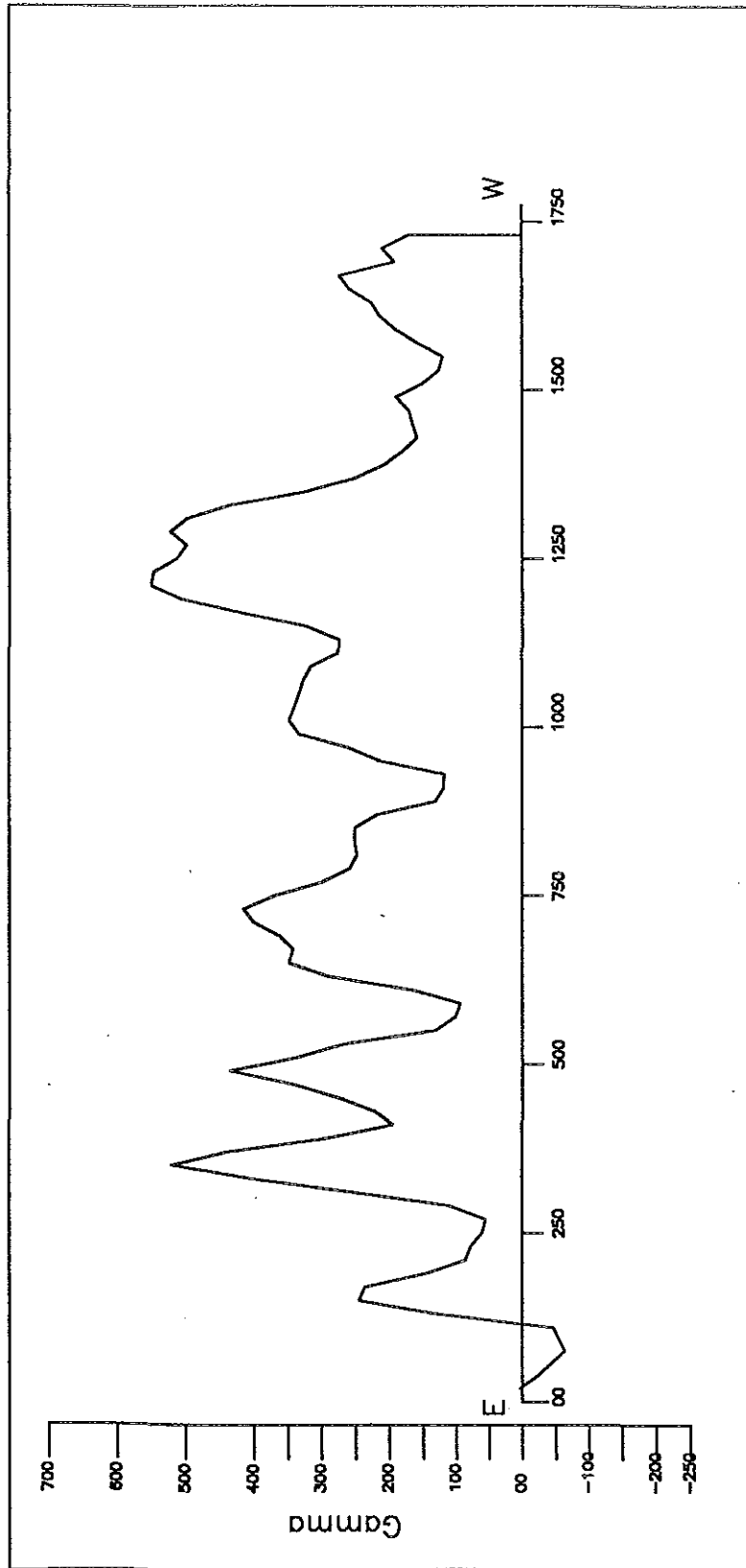


Fig.16 Total field magnetic anomaly profile along line LM1.

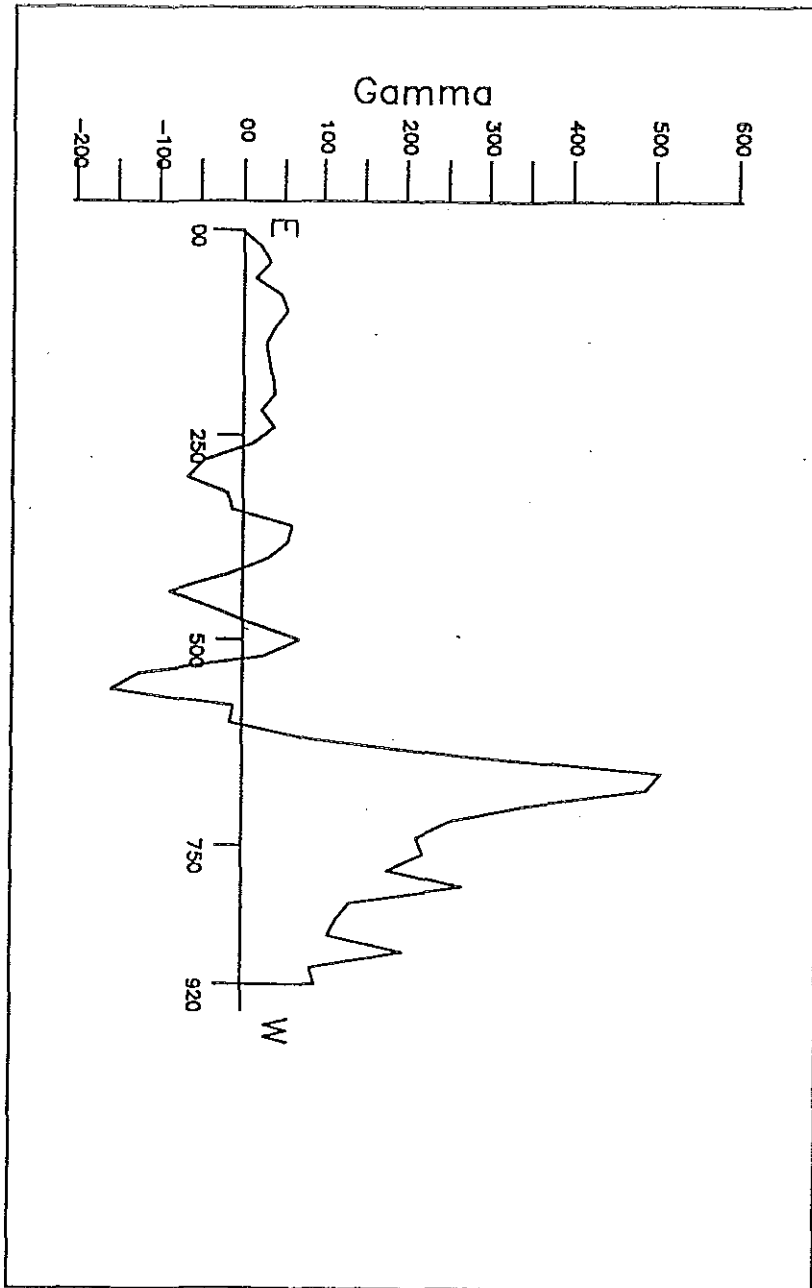


Fig. 17 Total field magnetic anomaly profile along line LM2.

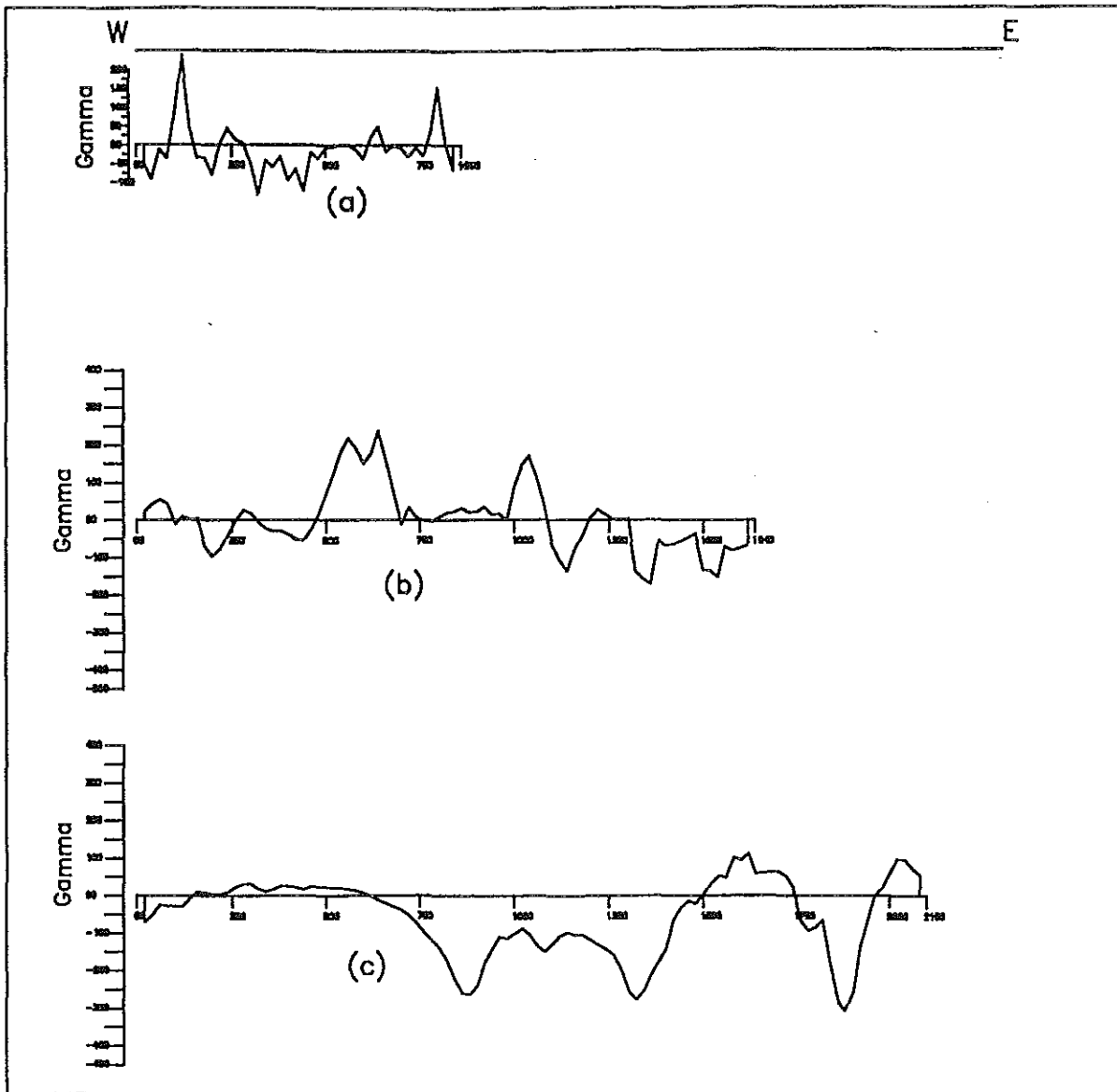


Fig.18 Total magnetic field anomaly profile along line LMV4 (a) line LMV3 (b) and LMV5 (c)

sounding survey. The low magnetic values observed at stations 900,1300 and 1900 may correspond to small fractures that are not delineated by the vertical electrical sounding (VES) survey. To the contrary, the high magnetic intensity recorded at station 1600 could be related with the response of hard welded tuff.

In addition to the information obtained from the total magnetic field anomaly profiles explained above the total field anomaly profiles explained above the total field magnetic map (fig.19) of themethehara area clearly shows a NNW and SSE trending fault in the NW part of the lake.

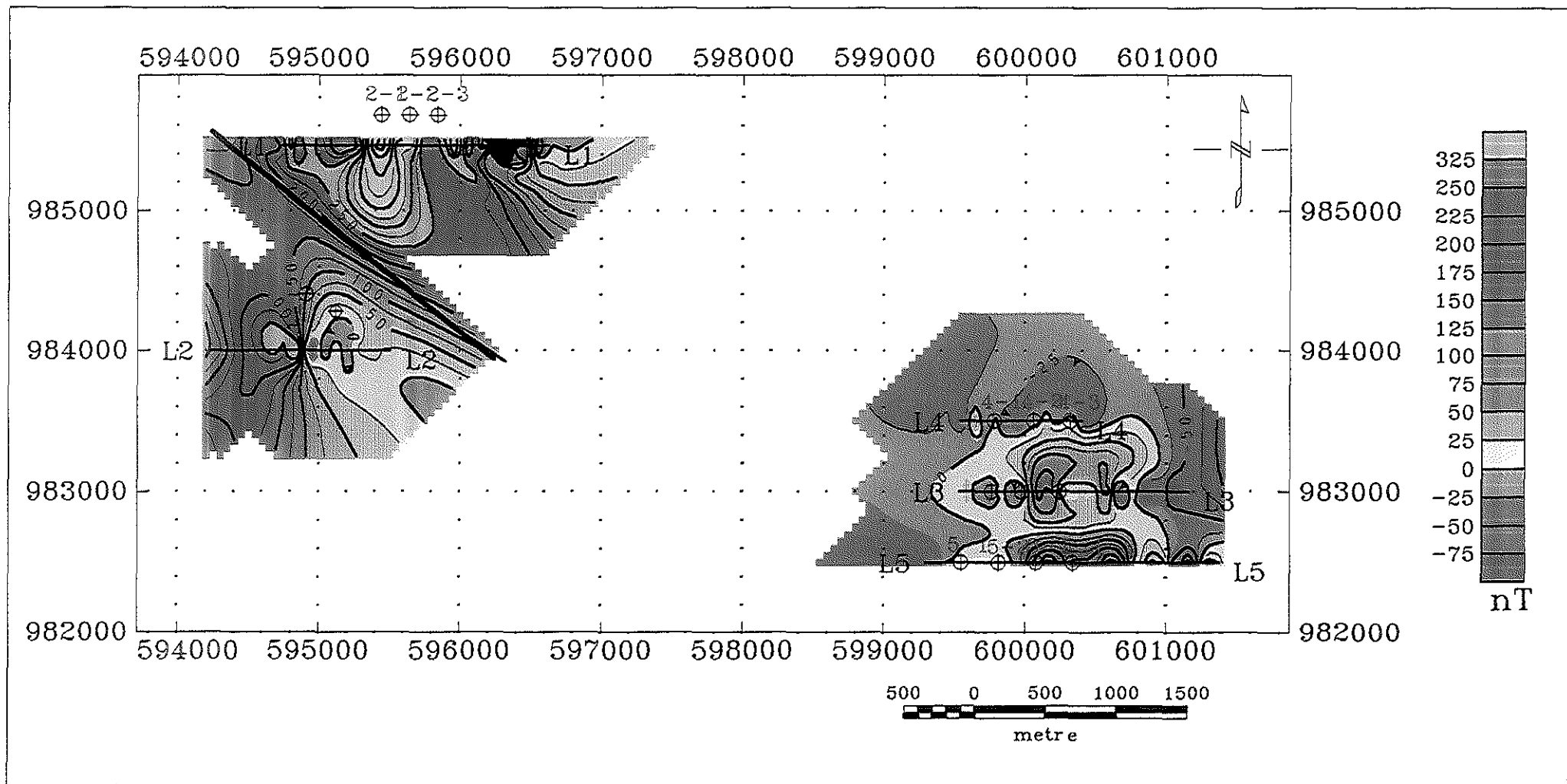


Fig. 19 Total field Magnetic map of Methara area

7. CONCLUSIONS AND RECOMMENDATIONS

7.1 CONCLUSIONS

The result of the magnetic survey conducted along line LM₂ (Fig. 17) shows a probable fault region, which may be the extension of the NNE-SSW trending faults observed from the geologic map. The vertical electrical sounding (VES) result obtained along LV₁ (Fig. 7) clearly shows uniform and low resistivity saturated horizon (about 2.5 0m-m) due to the intrusion of the saline lake water into the surrounding in addition to the circulation of groundwater into the area through the inferred faults and fractures.

The magnetic survey conducted in the NW of Lake Beseka along line LM₁ (Fig. 16) has outlined the existence of exposed or shallow depth volcanic rocks. As it is obtained from the vertical electrical sounding (VES) result along LV₂ (Fig. 8) in this region, the low resistivity layer appears to have a vast water bearing horizon. It accumulates groundwater draining probably from the Fentale Mountain and the western side of the survey area through these faults and fractures. As observed from the total field magnetic map (fig.19) in NW of the lake, a NNW and SSE trending fault is identified that may intersect the NNE and SSW trending faults through which the thermal springs apparent in the area may come to the surface.

The result of the vertical electrical sounding survey conducted in NE of Lake Beseka shows that the groundwater table lies in the depth range of about 2 to 16 m. The resistivity of the different aquifer systems is low in the vicinity of the lake and increases as one goes away from the lake, which is a clear indication of the intrusion of the saline lake water into the surrounding. This

result is in agreement with the previous geophysical work conducted in the SE part of the lake (E.I.G.S, 1998)

Even though the magnetic survey result along line LMV₄ doesn't show a clear fractured zone, the total magnetic field anomaly profile (Fig. 18) and the total magnetic field map (Fig. 19) indicate the presence of geologic structures (fractures and cracks) along lines LMV₃ and LMV₅.

Thus, the geophysical surveys conducted around the selected sites have succeeded in determining the depth to the top of the saturated zone, outlining probable faults (fractures and fissures) and identifying the general characteristics of the subsurface geology as given in the figures. But the results of the resistivity surveys show that no input of water to the lakes is possible from the adjacent farmlands, as the water table gets deeper as one goes away from the Lake. To detect the direction of groundwater flow long traverse geophysical surveys should be conducted beginning from the lake to a further distance away from it.

7.2 RECOMMENDATIONS

The problem of the Beseka Lake level rise has been a national problem for the last two-three decades. Eventhough different remedial measures have been taken at different times based on the previous studies, none of them have brought an everlasting solution. If an immediate remedial measure is not taken in due time for this problem, the most important lines of communication, railway and highway will be closed. Since the lake water is invading farm and grazing lands and the town of Methehara with an elevation difference of only a few meters our economic benefit from the area will be interrupted.

Thus, supplementary detailed geophysical work should be conducted in the area in addition to the geological and hydrogeological studies to obtain sufficient subsurface information. To get a complete information about the sources and the causes of the lake level rise the following recommendations are drawn:

1. Since it is impossible to cover the whole area and carry out a ground geophysical survey along inaccessible areas airborne geophysical surveys should be conducted in the area.
2. To obtain a reliable accurate information regarding the continuity of subsurface structures (faults) and groundwater flow direction an integrated remote sensing geological mapping, tectonic and geophysical mapping should be conducted in the area.
3. Further more the chemistry (isotope studies) of the lake water should be studied to identify the source that contributes to the lake level rise.

REFERENCES

- Asfaw L.M and kebede F. An Earthquake swarm from the Northern part of the Wonj Fault Belt. In proceedings of the 1st International symposium on crustal movement in Africa, UN-ECA, Addis Ababa.
- Battacharya P.K. and.Patra H.P., 1968. Direct current Geoelectric Sounding. Indian Institute of technology.
- Dipaola G.M., 1970. Geological-Geothermal Report on the central part of the Ethiopian Rift vally including the Tendaho-Assiata and Gawani, Fentale and petrographic Descriptions.
- Dobrin M.B. and Svit C.H., 1988. Introduction to geophysical Prospecting,Mcgraw Hill Inc. Singapore
- Edward L.S., 1977. Amodified pseudosection for resistvity and IP-Geophysics, V. 42, 1020-1036.
- Ghosh D.P., 1971a. The application of linear filter theory to the direct interpretation of geoelectrical resistivity measurements. Geophysical prospecting, V.19.
- Gibson, I.G. , 1970. Quaternary volcanism in the main Ethiopian Rift, 14th Annual Report, Reasearch Institute of African Geology, University of Leeds, England.
- Humel J.N, 1932. A theoretical study of apparent resistivity in surface potential methods. Trans, V.27, P.677-690.
- Kazmin V., 1975. Explanation of the Geological map of Ethiopia. Ethiopian Institute of Geological surveys. Bulletin No. 1,00-1-14.
- Kazmin V., Seife M., Berhe, Nicoletti M, Petrucciani C., 1980. Evolution of the Northern part of the Ethiopian Rift, Int. Meet. Geodynamic Evolution of the Afro-Arabic Rift system, ACC, Naz. Lincci, 275-291.
- Kazmin, V and Sief, 1978. Geology and development of the Nazreth Area Northern Ethiopia Rift, Un plished tech. Report,Ethiopian Institute of eological surveys, Addis Ababa.

- Keary P. and Brooks M., 1984.** An Introduction to Geophysical Exploration. Black well scientific publications, Oxford London, Edinburgh.
- Ministry of Water Resources, 1997.** Terms of Reference for the Study of Lake Beseka Continuous Level Rise Report, Addis Ababa
- Ministry of Water Resources, 1997.** Appraisal Report on the Continuous Rise of the Beseka Lake Level, Addis Ababa.
- Ministry of Water Resources (MoWR), 1998.** Regional Geology of Lake Beseka Area, Addis Ababa.
- Mohr P.A. (1971).** The Geology of Ethiopia. Addis Ababa University Press.
- Mooney H.M. and Wetzel W.W., 1956.** The potential about a point electrode and apparent resistivity curves for a two, three and four layered earth. The University of Mannesota press, Minneapolis.
- Nettelton , L.L, 1954,** Regionals , Residuals and structures : Geophysics, V.19, 1-22.
- Orellana E. and Mooney H.M., 1966.** Master tables and curves for vertical electrical sounding over layered structures. Interciencia, Madid.
- Parasnis D.S., 1986,** principles of applied Geophysics (4th edition). Chapman and Hall, London.
- Pekeris, C.L. (1940).** Geophy. 5,31-42
- Schlumberger. ,1955.** Generale de geophysique . France
- Scintrex Geophysical and Geochemical Instrumentation and services, 1988.** MP-3/4 Version R₁ 782 700 proton magnetometer systems operational manual.
- Slichter L.B., 1933.** The interpretation of the resistivity prospecting method for horizontal structures. Physics, V.4, P.307-322.

Shimelis Belayneh et al ,E.I.G.S (1988). Geophysical Investigations for the Lake Beseka study and Design project. Addis Ababa.

Telford W.M., 1990, Applied geophysics (2nd Edition), Cambridge University Press, USA